geosciences

MDPI

Article

First Geoarchaeological and Archaeometric Investigation at the Lucanian (4th–3rd Century BCE) Site of Laurelli (Cilento, Vallo di Diano and Alburni UNESCO Global Geopark—Southern Italy)

Ettore Valente [1,*], Antonia Serritella [2], Maria Luigia Rizzo [2], Michele Scafuro [2], Carlo Scirocco [1], Domenico Guida [3,4], Mario Valiante [3], Chiara Comegna [2], Giuseppina Balassone [1,5], Alberto De Bonis [1,5], Celestino Grifa [5,6] and Elda Russo Ermolli [1]

[1] Department of Earth, Environment and Resources Sciences, University of Naples Federico II, 80126 Naples, Italy; geocasci@gmail.com (C.S.); balasson@unina.it (G.B.); alberto.debonis@unina.it (A.D.B.); ermolli@unina.it (E.R.E.)
[2] Department of Cultural Heritage Sciences, University of Salerno, 84084 Fisciano, Italy; aserritella@unisa.it (A.S.); marizzo@unisa.it (M.L.R.); mscafuro@unisa.it (M.S.); ccomegna@unisa.it (C.C.)
[3] Department of Civil Engineering, University of Salerno, 84084 Fisciano, Italy; dguida@unisa.it (D.G.); mvaliante@unisa.it (M.V.)
[4] Consorzio Inter-Universitario per la Previsione e Prevenzione dei Grandi Rischi (CUGRI), University of Salerno, 84084 Fisciano, Italy
[5] Inter-University Center for Research on Archaeometry and Conservation Science (CRACS), University of Naples Federico II, University of Sannio, 82100 Benevento, Italy; celestino.grifa@unisannio.it
[6] Department of Science and Technology, University of Sannio, 82100 Benevento, Italy
* Correspondence: ettore.valente@unina.it

Abstract: The Lucanian site of Laurelli represents one of the largest, still poorly investigated, pre-Roman archaeological sites of the Cilento, Vallo di Diano and Alburni Geopark (southern Italy). The site lies on a large, low-relief surface in the upper portion of the Serrapotamo River basin, a right tributary of the Bussento River. Geomorphological, stratigraphical, archaeobotanical and archaeometric analyses were carried out to understand the following: (1) the choice to settle at the site of the town of Laurelli; (2) the origin of the raw material used to build the town; (3) the vegetation present during the lifetime of the town; and (4) the causes of its abandonment. The results indicate that the site was chosen because it was almost stable from a geomorphological point of view, not being affected by deep landslides. Further investigations are needed to unravel the possible occurrence of flooding as a causative event for the abandonment of Laurelli. *Carpinus* was widespread and used as a fuel for iron production, but the areas from which the iron was extracted have not yet been discovered. The multidisciplinary approach adopted is suitable for application in other archaeological areas worldwide.

Keywords: geomorphology; morphostratigraphy; archaeobotany; archaeometry; iron production; geosite

check for updates

Academic Editor: Lev V. Eppelbaum

Received: 22 November 2024
Revised: 4 January 2025
Accepted: 7 January 2025
Published: 12 January 2025

Citation: Valente, E.; Serritella, A.; Rizzo, M.L.; Scafuro, M.; Scirocco, C.; Guida, D.; Valiante, M.; Comegna, C.; Balassone, G.; De Bonis, A.; et al. First Geoarchaeological and Archaeometric Investigation at the Lucanian (4th–3rd Century BCE) Site of Laurelli (Cilento, Vallo di Diano and Alburni UNESCO Global Geopark—Southern Italy). *Geosciences* **2025**, *15*, 25. https://doi.org/10.3390/geosciences15010025

1. Introduction

The Cilento, Vallo di Diano and Alburni (CVDA) Geopark (Campania Region, Southern Italy) is one of the four United Nations Educational, Scientific and Cultural Organization (UNESCO) international designations of the Cilento, Vallo di Diano and Alburni National Park (CVDANP). It is also one of the largest Italian geoparks, covering an area of 1841 km^2

with a population of approximately 280,000 inhabitants. It has obtained several international endorsements since its foundation and was established by a National Law in 1991 as a National Park. It was included in the Man and Biosphere List by UNESCO in 1997, and in the World Heritage List by UNESCO in 1998. These endorsements are based on the long term "cultural landscape" concept, showing "*outstanding value that has evidence of human occupation dating from 250,000 years ago... successively occupied over time by farmers during the Neolithic period, by Bronze and Iron Age societies, Etruscans, Greek colonists, Lucanians, and was eventually incorporated into the Roman territory in the 3rd century BC*" (https://whc.unesco.org/en/list/842/documents/; accessed on 15 November 2024). The CVDANP was recognized as a European and Global Geopark in 2010, and it was included in the UNESCO Global Geopark network in 2015 [1]. A geopark is defined as "*a territory with well-defined limits that has a large enough surface area for it to serve local economic development. The Geopark comprises a number of geological-paleontological heritage sites of special scientific importance, rarity or beauty; it may not be solely of geological-paleontological significance but also of archaeological, ecological, historical or cultural value*" [2]. This definition implies a strong connection between geological-paleontological and cultural-archaeological sites and the development of the local economy. UNESCO Global Geoparks are "*single, unified geographical areas where sites and landscapes of international geological significance are managed with a holistic concept of protection, education and sustainable development*" [3]. The CVDA UNESCO Global Geopark includes both geological-paleontological sites (namely geosites and geomorphosites) and archaeological sites. Despite the scientific relevance of geosites and geomorphosites, as has been discussed in international papers [1,4–7], conference proceedings and national papers ([1] and references therein), the connection between geosites and archaeological sites has not been thoroughly investigated until now.

Among the known archaeological and historical sites are the famous sites of Paestum, Elea-Velia and the Padula Charterhouse (Figure 1). The sites of Paestum and Elea-Velia form the Archaeological Park of Paestum-Velia, which was visited by approximately 500,000 tourists in 2023 [8]. Both sites are included in the CVDA geopark list of geosites [9] and in proposed geoitineraries [6,7]. This strong connection between archaeological sites and geological-geomorphological features is due to the use of local rock types as the raw material to build the towns, as well as to the relationship between landscape modification and human occupation phases. These connections are discussed in several scientific papers [10–13]. The Padula Charterhouse is a wonderful example of baroque architecture in southern Italy, covering an area of approximately 50,000 m^2. This site is located on the western piedmont of the Maddalena Mts., along the eastern side of the Middle Pleistocene Vallo di Diano intramontane lacustrine basin. Its location made the site prone to suffering alluvial events [14]. The most recent and destructive event was the 1857 alluvial flood that led to the accumulation of a couple of meters thick alluvial deposits covering part of the charterhouse [15].

Besides these famous archaeological sites, the CVDA geopark has hosted human occupation since prehistoric times, as is evidenced along the coastal area of the geopark [16,17].

Other examples of archaeological sites testifying to well organised human societies are the Lucanian sites of Roccagloriosa and Laurelli, in the southern portion of the CVDA geopark (Figure 1). In this paper we focused our analysis on the site of Laurelli. Here, archaeological investigations are in progress, and a comprehensive geoarchaeological analysis has not been carried out so far. Archaeological excavations at Laurelli started in the 1990s, were halted in the early 21st century and were restarted in the last ten years. The site of Laurelli is located in the Middle Bussento Karst System, which is one of the geosites of the CVDA geopark and whose geotourism potential has already been assessed [1]. Nevertheless, the analysis by Valente et al. [1] did not consider the archaeological site of

Laurelli because of the embryonic stage of the geoarchaeological research. Since that time, the geoarchaeological analysis of the Laurelli site has been more thoroughly developed. These analyses have been carried out to provide answers to some open questions, such as the following: (1) why was this the site chosen to settle Laurelli? (2) where did the raw material for building the town come from? (3) what type of vegetation was present during the life of Laurelli? and (4) why was the town abandoned?

In this paper, we provide geomorphological, stratigraphical, archaeobotanical and archaeometric data gathered with the aim of answering some of the aforementioned questions. We are also confident that such an approach may be adopted in other sites worldwide.

2. Study Area

2.1. Geological Setting

The study area lies in the southernmost portion of the Southern Apennines, a NE-verging fold and thrust belt formed by the Neogene convergence between the African and Eurasian plates [18,19] (Figure 1). The tectonic evolution of the chain caused the juxtaposition of tectonic units accumulated in different geodynamic settings [20–26], most of which are exposed in the surroundings of Laurelli. There, Jurassic to Eocene carbonate units are overthrust by Eocene to Lower Miocene internal oceanic units. The latter are covered in disconformity by both Miocene Flysch units and Cilento wedge-top units. Ubiquitous Quaternary continental deposits mainly accumulated in the river valleys and cover the above-mentioned units (Figure 2). These tectonic units are made of different rock types that react non-homogeneously to erosional and weathering processes. It follows that the study area exhibits topographic peaks, where "resistant" rock types crop out (e.g., carbonate and arenaceous units), and a smoother landscape, where "softer" rock types crop out (e.g., marly-clayey units).

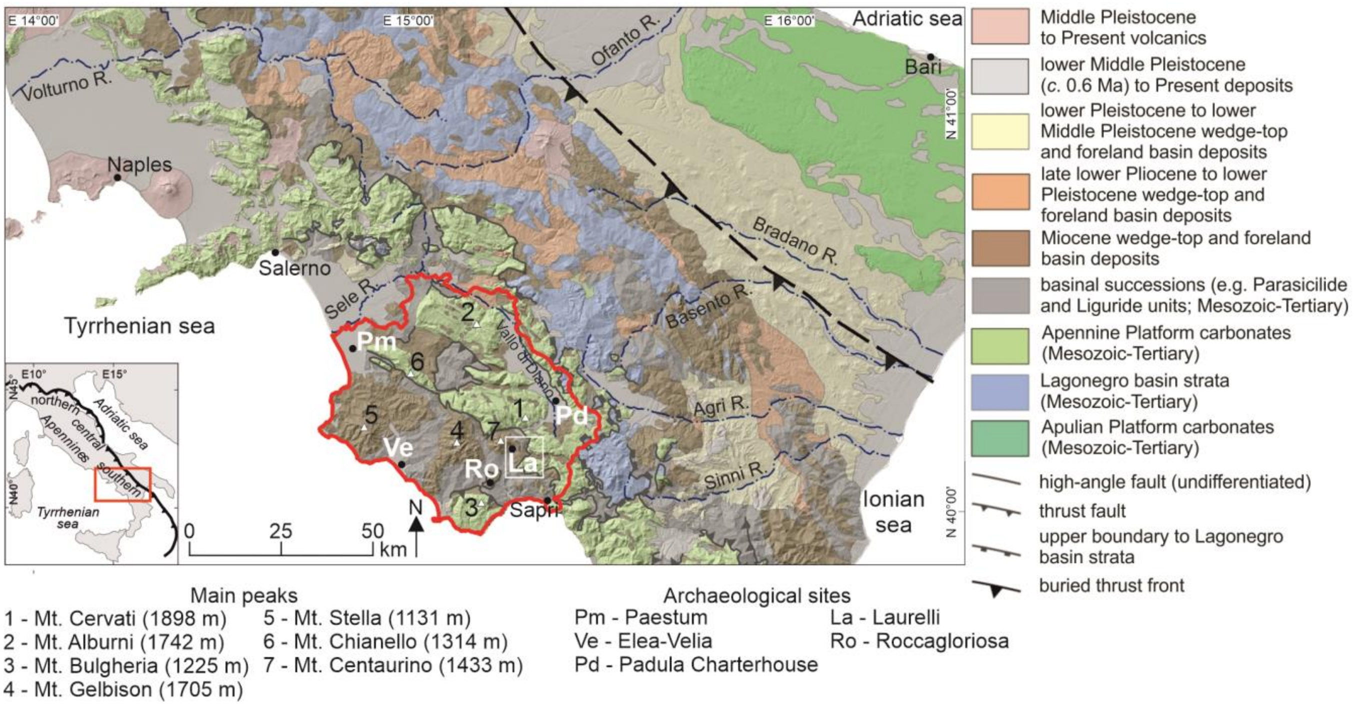

Figure 1. Geological map of the Southern Apennines (modified from [7]), with the location of the Cilento, Vallo di Diano and Alburni UNESCO Global Geopark (red line). White box in the southeastern portion of the CVDA geopark refers to Figure 2.

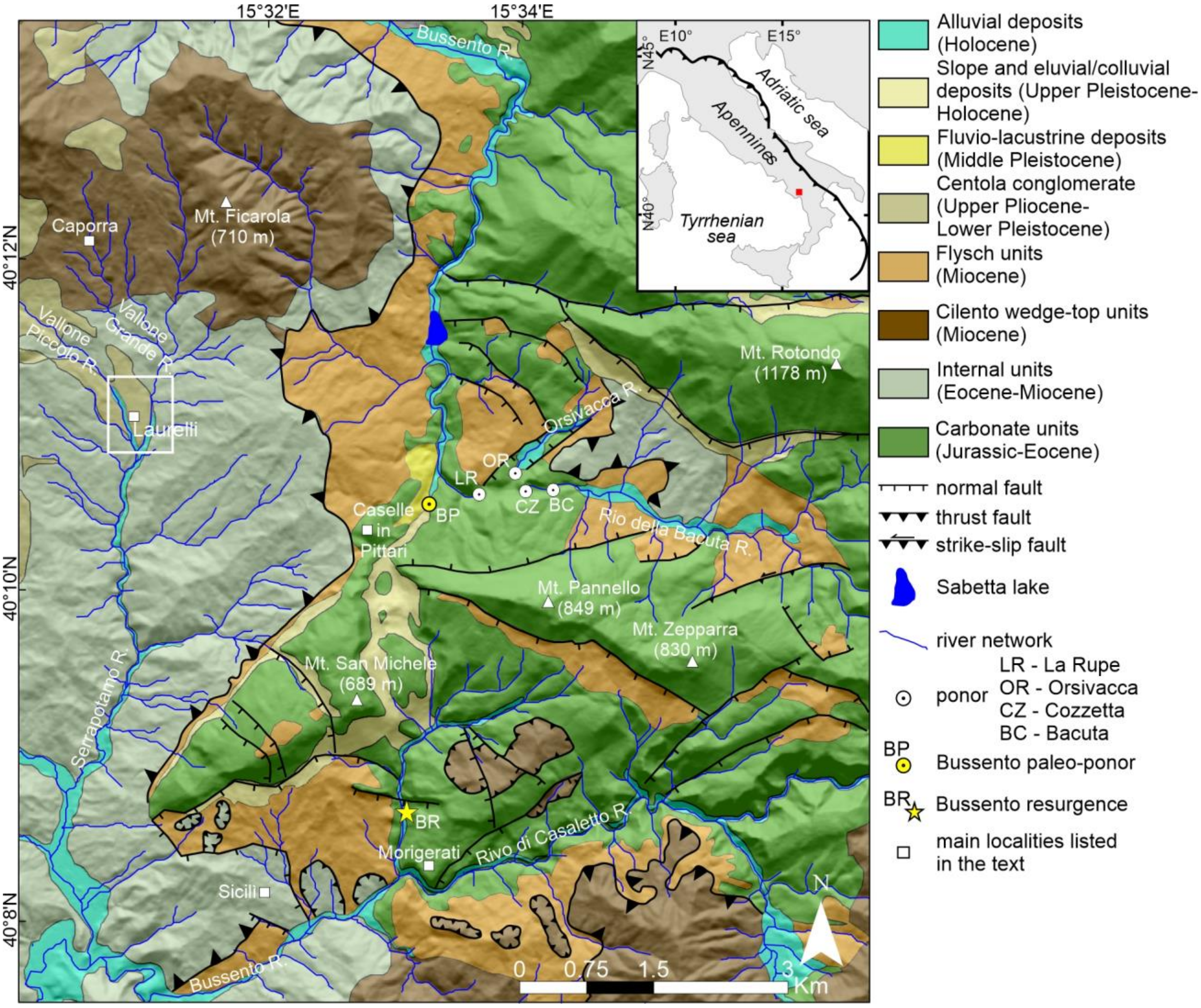

Figure 2. Geological map of the study area (modified from Valente et al. [1]). The white box indicates the Google Earth orthophoto shown in Figure 3. The red box in the inset map shows the location of the study area within the Apennines chain.

More precisely, Jurassic to Eocene carbonate successions crop out to the east of Laurelli and correspond to the highest topographic peaks (i.e., Mt. San Michele, Mt. Pannello and Mt. Rotondo; Figure 2). They are made of inner-platform carbonate very rich in fossils (rudists and gastropods) passing upward to open shelf limestone with interlayered marls and clays [27]. Internal units crop out near Laurelli (Figure 2) and are made of clays with interbedded quartz-rich and feldspar-rich sandstones passing upwards to calcilutites, calcarenites and calcirudites with cherty lists and nodules and with interbedded quartz arenite and marls strata [27]. Miocene Flysch Units consist of a fining upward sequence of thrust-top deposits [27]. They crop out to the east of Laurelli and are found either in some topographic lows (e.g., the Bussento River and the Rio della Bacuta River valleys; Figure 1) or locally resting on the carbonate units (e.g., on top of Mt. San Michele; Figure 1). The Miocene Cilento wedge-top units consist of a coarsening upward sequence of wedge-top basins [27]. Quaternary deposits include both recent alluvial deposits accumulated along the main valleys (e.g., the Serrapotamo River, the Bussento River and the Rio della Bacuta River valleys; Figure 4A) and slope deposits accumulated at the toe of some carbonate ridges (e.g., Mt. San Michele and Mt. Rotondo; Figure 2). Furthermore, ancient fluvial deposits also rest on the slopes carved both in the Cilento units and in the internal units, and locally form remnants of large low-relief surfaces. These ancient fluvial deposits, previously known collectively as the Centola Conglomerate (Figure 4B), have been recently renamed the Rofrano Synthem and Faraone Synthem on the official national geological map [27]. They testify to a multi-stage fluvial-gravitational valley-filling evolution during the stadial age of the study area, initially described as "stone stream" deposits by Guida et al. [28].

The archaeological site of Laurelli is located in the upper portion of the Serrapotamo River basin, which is a right tributary of the Bussento River (see Figure 2 for reference). In the upper portion of the Serrapotamo River basin, alluvial deposits occur at the valley's bottom, while the Centola Conglomerate-Faraone Synthem, or stone stream deposits, form large low-relief surfaces that hang about ten meters above the present-day riverbed. The largest of these surfaces, locally named the "Pianoro Inferiore", occurs at the confluence of the Vallone Piccolo and Vallone Grande rivers, which are tributaries of the Serrapotamo River, and hosts the archaeological site of Laurelli (Figure 4).

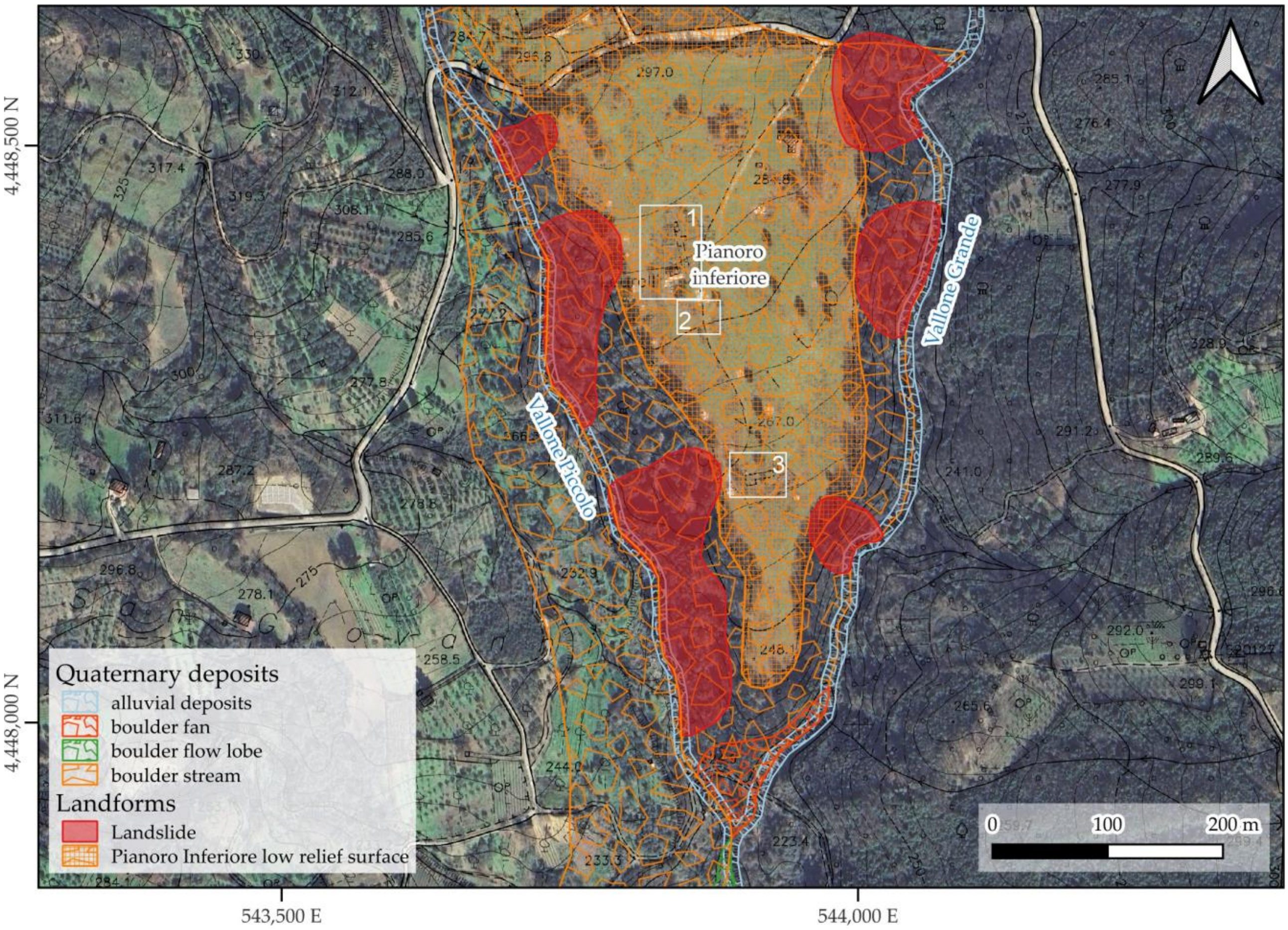

Figure 3. Quaternary units and geomorphological features of the "Pianoro Inferiore" low-relief surface. White boxes indicate the areas under archaeological investigation. 1-Plateia A; 2-Metallurgic workshop; 3-House of Coins.

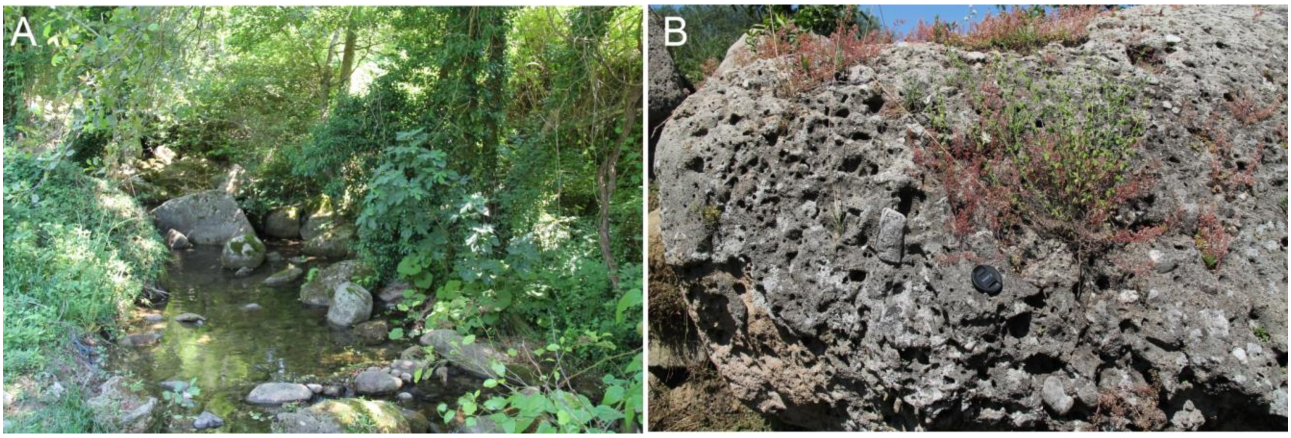

Figure 4. (**A**) Alluvial deposits along the Vallone Piccolo River valley bottom, with the diffuse presence of large (cubic meters) boulders; (**B**) Detail of a cubic meter boulder accumulated on a low-relief surface near the archaeological site of Laurelli. These large boulders are made up of the Centola Conglomerate/Faraone Synthem and derive from the eastern slope of Mt. Centaurino.

2.2. Archaeological Setting

The Lucanian site of Laurelli is located a few kilometres to the north-west of the modern village of Caselle in Pittari (Figure 2), and it occupies a privileged location between the sea and the Vallo di Diano (Figure 1). It developed between the second half of the 4th century BCE and the mid-3rd century BCE on a very large, low-relief surface known as the Pianoro Inferiore (Figure 3), which is bordered by perennial rivers that, at least in part, provided a water supply. The steep scarps bounding the Pianoro Inferiore not only defined the perimeter of the settlement but also ensured its natural protection, justifying the absence of a surrounding wall.

Today, the Pianoro Inferiore is divided into two parts by a modern rural road; stratigraphic investigations have been carried out exclusively in the southernmost sector, which corresponds to the limits of the state-owned Archaeological Park. Surface surveys in the northernmost portion of the Pianoro Inferiore confirmed the extension of the settlement into this area as well [29]. Excavations took place from 1990 to 2006 under the direction of the Archaeological Superintendence [30], and since 2014 have been carried out under the direction of the University of Salerno (Excavation Permit from the Ministry of Culture, rep. 673 of 30/05/2022) [29,31–33].

The southernmost sector of the Pianoro Inferiore served as an access point to the site from the coast. Here, a lookout point has been identified at the confluence of the Vallone Grande and Vallone Piccolo rivers, along with a large flat and paved space along the Vallone Grande River valley, which may have served as a landing site.

Archaeological and geophysical investigations [34] have revealed that the settlement is characterized by a regular layout, with roads dividing the blocks. A wide N–S oriented plateia, about 10 m wide, crosses the entire plateau and is intersected every 42 m by narrow streets (stenopoi) that are approximately 4 m wide (Figure 5). On the eastern side of Plateia A, the northernmost block contains Building V, of which the complete plan has not yet been reconstructed. On the same side, in the next block to the south, the "House in Checkerboard Technique" is located—a residential building of over 500 square meters, with a paved ramp and rooms arranged around a central courtyard. Further south, the adjacent third block contains the "House with the Metallurgical Workshop", whose productive function related to ironworking is evidenced by the discovery of a space dedicated to the purification of raw ore and several kilograms of iron sponges [35], which are currently under analysis.

Figure 5. Orthophoto of the *plateia* area in the central portion of the Pianoro Inferiore. The orthophoto is derived by an airborne drone investigation.

On the opposite side of Plateia A, the House in Checkerboard Technique occurs, which contains a complex extending over two terraces, separated by a change in elevation. The upper terrace features a quadrangular structure made of pebbles, while the lower terrace consists of a series of covered and uncovered spaces, creating a distinctive layout that, along with the movable finds, suggests a communal function for this area. A public space is also suggested by the dismembered remains of a fountain and the ring of a large well connected to it, found in an area not related to its original context to the north of the Archaeological Park.

In the southern part of the Pianoro Inferiore, the so-called "House of the Coins" was unearthed, named for a hoard of 20 silver coins [36] found in one of the rooms.

The level of complexity reached by the community, as expressed in the settlement system, is reflected in the variety of vessels found across all the building. These vessels bear inscriptions in both the Oscan and Greek alphabets, and possibly even in archaic Greek, alongside symbols likely related to arithmetic calculations.

3. Materials and Methods

3.1. Geomorphological Analysis

The main landforms of the study area were identified by means of classical geomorphological analysis of detailed-scale topographic maps coupled with field surveys. The topographic maps used in this study are the 1:5000 scale maps of the Campania Region (available online at https://sit.regione.campania.it/WebGisOD/mapviewer.jsf?width=1163&height=506&firstpageload=true; accessed on 10 October 2024). These maps have also been used to derive a 5 m Digital Terrain Model (DTM) that served as base map for mapping the recognised landforms. The 5 m DTM has also been modelled to obtain a slope map to recognize elementary landforms [37,38] and to reconstruct the river network. The latter has been obtained using the hydrology tools of ArcGis (Esri ©, Redlands, CA, USA).

Among the recognised landforms, landslides diffusely affect the hillslopes and scarps of the study area. The recent development of studies related to the hydrogeological risk by local authorities has allowed the production of detailed-scale maps (1:5000 scale) showing the distribution of landslides. These data are available online (https://www.distrettoappenninomeridionale.it/piano-stralcio-assetto-idrogeologico-rischio-da-frana/uom-regionale-sinistra-sele-ex-adb-reg-campania-sud-ed-interr-sele-ex-adb-reg-sinistra-sele/; accessed on 10 October 2024); the shapefile of the landslides was downloaded from this link and was included into the geomorphological map of the study area.

Furthermore, we obtained a detailed DTM of the Pianoro Inferiore area through an airborne drone investigation. This DTM has a horizontal resolution of 8 cm and was used to identify landforms of the Pianoro Inferiore that had not been recognised through the classical geomorphological approach. We also derived a visibility map of the Laurelli area, centred in the Pianoro Inferiore, to verify a possible visual connection with other archaeological sites (e.g., the Roccagloriosa site). We adopted a 10 m DTM (TINItaly project; https://tinitaly.pi.ingv.it/Download_Area1_1.html [39]; accessed on 10 October 2024) to derive this map and obtained it using the visibility tool of ArcGis.

3.2. Stratigraphical Analysis

As part of the Caselle in Pittari conservation and enhancement project, 50 boreholes were drilled on the Pianoro Inferiore, with the aim of investigating the nature and thickness of the deposits covering the archaeological remains. The location of the boreholes (Figure 6A), whose depth is 4 m, was decided by the Superintendence Authority based on the results of preliminary archaeological and georadar surveys. Core drilling was carried out in the summer of 2000 using an MK 400 rotary probe and a 3-m long core barrel with diameters of 114 mm and 95 mm. Cores were stocked in cataloguing boxes and described, in a good degree of detail, by the drilling company.

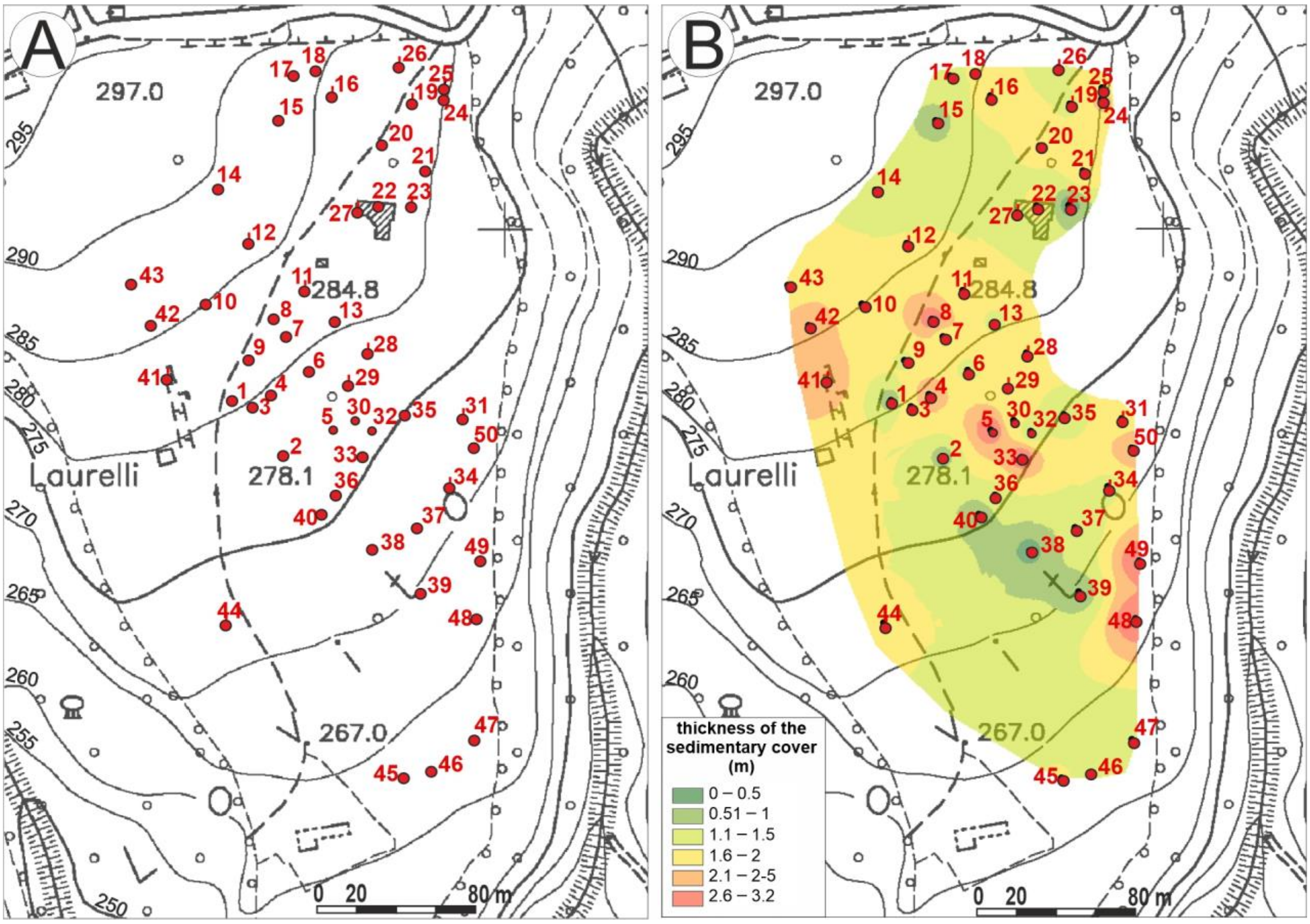

Figure 6. (**A**) Location of the 50 cores drilled on the Pianoro Inferiore of the Laurelli archaeological site; (**B**) map showing the thickness of the sediments covering the bedrock. The base map is the 1:5000 scale map of the Campania Region.

3.3. Wood and Seed Analysis

Sediment samples were collected by archaeologists during excavations in 2021, 2022 and 2023 from two different trenches (7 and 12) and pertaining to different UUSS (Archaeological Stratigraphic Units). In 2021, two samples were collected from trench 7: one from the level of mopping up of the trench and one from a single layer (US 1085) interpreted as a level of abandonment. In 2022, three different layers were collected from trench 12: US 1098, interpreted as colluvial sediment covering a rammed earth floor; US 1107, interpreted as an accumulation of sediment and stones possibly related to the collapse of an ancient structure; and US 1104, interpreted as an accumulation of stones related to the collapse of ancient architectural elements. In 2023, five samples were collected at different depths from US 1125 (trench 7), interpreted as a level related to the working phases of a metallurgical workshop.

The 10 collected samples (Table 1) were sieved in water or dry-sieved, using two mesh sizes (0.5 mm and 0.2 mm) to recover all the carbonized seeds and wood fragments. All samples from US 1125 were first dissolved in water and then sieved because they were very compact, and the carbonized wood fragments were strongly embedded in it. The residues of all samples were screened under a stereomicroscope to recover all the finds.

Table 1. Details of the results of the anthracological analysis.

Sample	US	Trench	Year of Collection	Anthracological Remains	Average Size (cm)	Genus/Species
1	1085	7	2021	9	0.5	*Ostrya/Carpinus*
				1	0.2	*Vitis vinifera* L.
2	"mopping"	7	2021	22	0.5	*Olea europea* L.
3	1098	12	2022	4	0.4	*Olea europea* L.
4	1107	12	2022	21	0.4	*Olea europea* L.
5	1104	12	2022	16	0.4	*Olea europea* L.
6	1125 (−18 cm)	7	2023	1	0.7	indetermined
7	1125 (−23 cm)	7	2023	16	0.4–1	*Ostrya/Carpinus*
8	1125 (−26 cm)	7	2023	4	0.4–1	*Ostrya/Carpinus*
9	1125 (−32 cm)	7	2023	11	0.4–1	*Ostrya/Carpinus*
10	1125 (−65 cm)	7	2023	1	0.3	indetermined

The analysis of the carbonized wood fragments was conducted by observing three sections of the wood under a reflected light microscope (rLM) using magnifications between 50 and 250 X. Identification was made with the support of wood anatomy atlases [40–43], a comparative collection (anthracoteque) and digital identification keys (INTKEY, INSIDEWOOD). The analysis of the seeds was conducted using a stereomicroscope, and identification was carried out via comparison with the seeds collection (carpotheque).

3.4. Iron Fragments Analysis

For a preliminary characterization of the iron-rich slags, four selected samples (# CIP1, CIP2, CIP5 and CIP6) were prepared as polished opaque mounts to analyse their microstructures. These samples were first studied by means of polarizing Optical Microscopy (OM), using a reflected light Laborlux 12 POL (Labexchange, Burladingen, Germany) polarizing microscope equipped with a Carl Zeiss Axiocam 105 color (5-megapixel resolution).

Mineralogical analyses were performed via X-ray powder diffraction (XRPD), using a Seifert–GE ID3003 diffractometer, with CuKα radiation, Ni-filtered at 40 kV and 30 mA, in the 3–80° 2θ range, with a step scan 0.02° and a time 10 s/step at the Department of Earth, Environment and Resources Sciences, University of Naples Federico II (Naples, Italy), using the RayfleX (GE) software package, version 2.337.

Micromorphological and qualitative-quantitative chemical analyses obtained via scanning electron microscopy with energy dispersive X-ray spectroscopy (SEM-EDS) were carried out using a JEOL JSM5310 electron microscope (JEOL, Japan) equipped with an Oxford energy dispersive spectrometry (EDS) INCA X-stream (Oxford Instruments, Abingdom, UK) pulse processor and the 4.08 version Inca software; the operating conditions were an acceleration voltage of 15 kV and a working distance of 20 mm. The reference standards used for quantitative microanalysis were minerals and pure metals.

Qualitative SEM-EDS investigations and elemental maps were also carried out with a Zeiss EVO HD15 instrument (Department of Science and Technology,University of Sannio, Benevento, Italy), coupled with EDS using an Oxford X-Max 80 instrument (Oxford Instruments, Abingdom, UK). The analytical conditions were as follows: 20 mm objective lens to specimen working distance and 15 kV accelerating voltage with a tilt angle of 0°.

4. Results

4.1. Landforms and Processes Affecting the Archaeological Area of Laurelli

The archaeological area of Laurelli is placed on the largest low-relief surface located in the upper portion of the Serrapotamo River basin, at the junction between the Vallone Grande and Vallone Piccolo rivers. This low-relief surface, named the Pianoro Inferiore, is carved in the Centola Conglomerate/Faraone synthem deposits (see Section 2), which locally crop out from the overlying sedimentary cover, and is limited by steep scarps (Figure 7A). These include both fluvial scarps and a degraded scarp. Fluvial scarps are from 5 m to 20 m high and are affected by small landslides, which mainly occur to the west of the Pianoro Inferiore. The degraded scarp limits the Pianoro Inferiore to the north and is 15 to 25 m high. This scarp separates the Pianoro Inferiore from another low-relief surface named the Pianoro Superiore. Archaeological data suggest that the town of Laurelli may also extend here, but this area has not been thoroughly investigated to date (Section 2.2). To the west of the Pianoro Inferiore, another elongated low-relief surface hosts the Necropolis of Laurelli (Figure 7A).

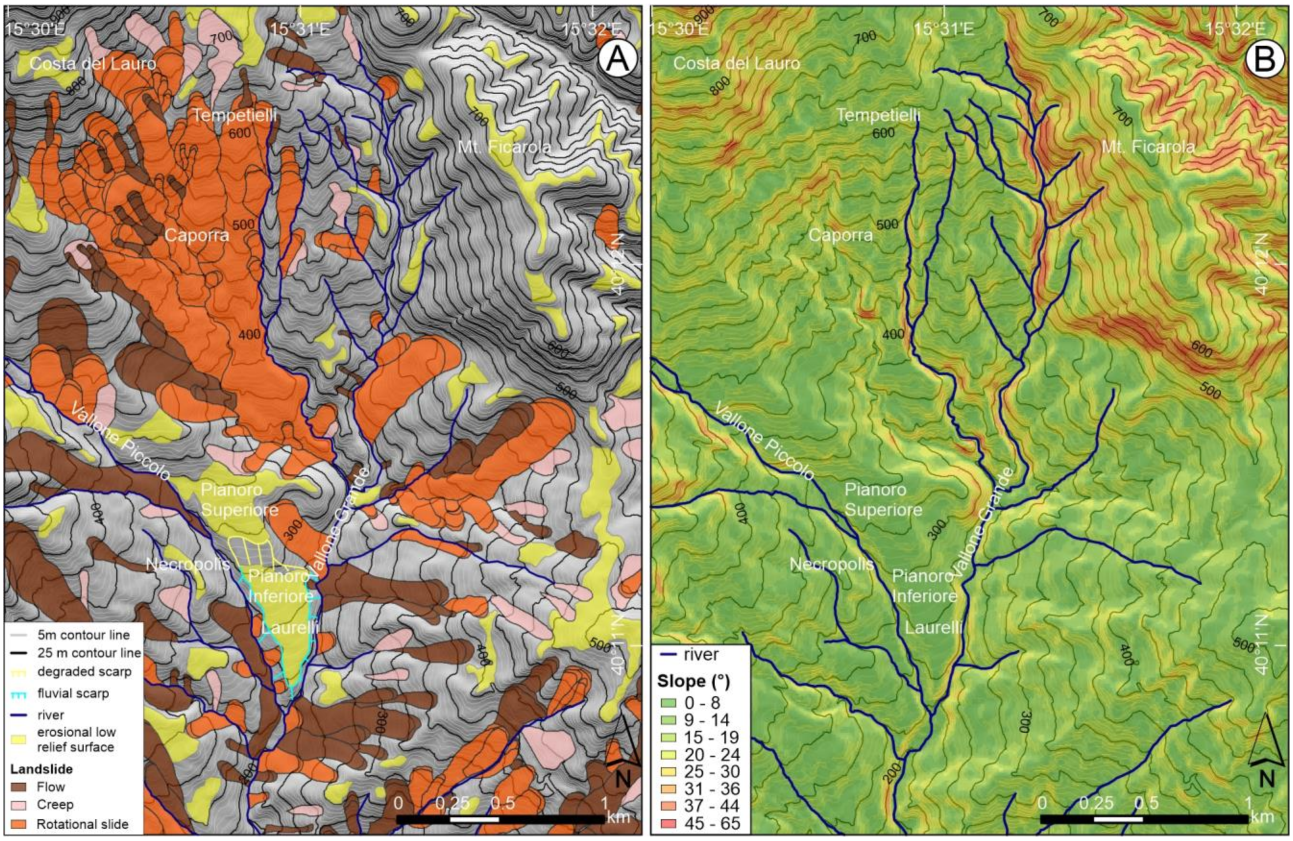

Figure 7. Geomorphological sketch (**A**) and slope map (**B**) of the upper portion of the Serrapotamo River basin hosting the archaeological area of Laurelli.

The Pianoro Inferiore, the Pianoro Superiore and the Necropolis are the largest low-relief surfaces preserved in this area. Other low-relief surfaces occur along the valley flanks and on top of some ridges. These surfaces are relatively small and are degraded because of the diffuse presence of landsliding (Figure 7A). Landslides vary in length from a few meters (i.e., along the western scarp of the Pianoro Inferiore) up to a couple of kilometres (i.e., in the Caporra area, to the north of Laurelli). Landslides include flow and rotational slides, but areas subject to creep have also been included. Due to its size and its representativeness, the Caporra landslide system (sensu [44]) has been interpreted as a moving geosite by Calcaterra et al. [45].

The slope map of Figure 7B shows slope values mainly in the range between 0° and 19°. These values are associated with the diffuse presence of clayey rock types related to the internal units (see Section 2). The lowermost slope values (0–8°) occur where the low-relief surfaces are preserved. Local increments in slope values occur where fluvial scarps are present. In the uppermost portion of the study area, slope exhibits its highest values, reaching a maximum of 65° in the Mt. Ficarola area. The increase in slope values along the flank of Mt. Ficarola is related to the outcrop of Cilento wedge-top units (see Section 2).

Further details about the features of the landscape in the Pianoro Inferiore area were obtained through an analysis of the 8 cm DTM. This DTM allowed reconstruction of a detailed topographic profile of the Pianoro Inferiore (Figure 8). The topographic profile highlights the occurrence of jumps ranging from tens of decimetres to 1 m in height that interrupt the quasi-flat morphology of the area. These local increases in slope are related to local outcrops of the Centola Conglomerate from the colluvial wedge. In some cases (e.g., in the House of the Coins area), these jumps have been used to locate the external walls of residential buildings (Figure 9).

4.2. Visibility Map

The point of view used to derive the visibility map has been placed on the Pianoro Inferiore (Figure 10). Areas visible from this point are shown in red on this map.

The visibility map shows that the location of the archaeological site of Laurelli allowed a visual connection with most of the Serrapotamo River basin and with part of the lower reach of the Bussento River basin. The view extends to the west up to the eastern flank of Mt. Centaurino, whereas the southern slope of Mt. Ficarola limits the view towards the north. To the east, the north-western side of Mt. San Michele is clearly visible from the Pianoro Inferiore, whereas just the westernmost part of Mt. Pannello is visible. The highest peaks in the lower reach of the Bussento River basin are visible from the Pianoro Inferiore, including the hilly ridge that hosts the archaeological site of Roccagloriosa. It is noteworthy that towards the south, the view also extends beyond the hydrographic basin of the Bussento River and reaches the northern slope of Mt. Bulgheria and the hills of Scario, close to the sea.

4.3. Thickness and Nature of the Deposits Covering the Archaeological Remains

From the observation of the core logs (Figure 11), the Quaternary bedrock on which the Laurelli site was built (1, 2, 3 in Figure 11) lies at shallow depths of approximately 0.5 to 3 m. Its top has been interpreted as the occupation level of the Laurelli settlement (10 in Figure 11). In most cores, the bedrock is covered by fine colluvial deposits (4 in Figure 11), ca. 0.5 to 2.5 m thick, in which frequent ceramic fragments and traces of carbonisation are found, together with decomposed plant remains. This level was interpreted as evidence of the abandonment phase of the settlement. In some cores (S24, S41, S42), it is covered by chaotically arranged stones, interpreted as structural collapses (6 in Figure 11). Remains of wall structures in their primary position have been recognised in cores S16, S35, S44 and S45. The topmost portion of all cores consists of soils, with varying thicknesses, in which reworked ceramic fragments are found. For the purpose of understanding how much the original morphology of the frequentation level has changed since the abandonment of the site, a map showing the thickness of colluvial deposits in the different sectors of the Pianoro Inferiore was constructed (Figure 6B).

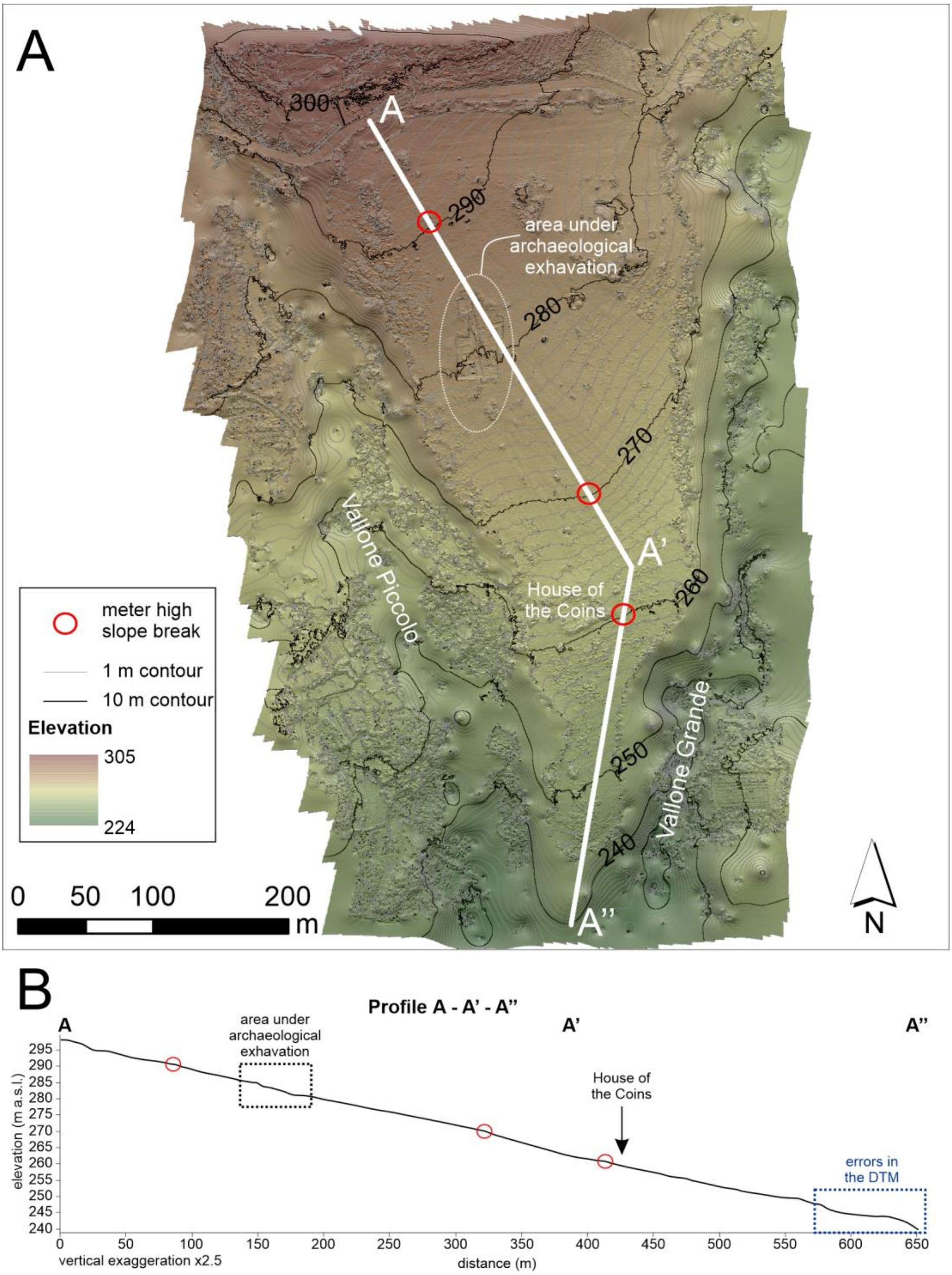

Figure 8. (**A**) Trace of the topographic profile (white line) constructed to highlight landscape features of the Pianoro Inferiore that are not detectable via the classical geomorphological analysis of a 1:5000 topographic map. The base map is an elevation map derived from an 8 cm DTM. (**B**) Topographic profile of the Pianoro Inferiore. Red circles indicate the meter-high slope breaks reported in map (**A**).

Figure 9. Photo of the House of the Coins area. Orange polygon is the 1 m high scarp that limits the area toward the north. Local outcrops of the Boulder Stream deposits are denoted by white circles.

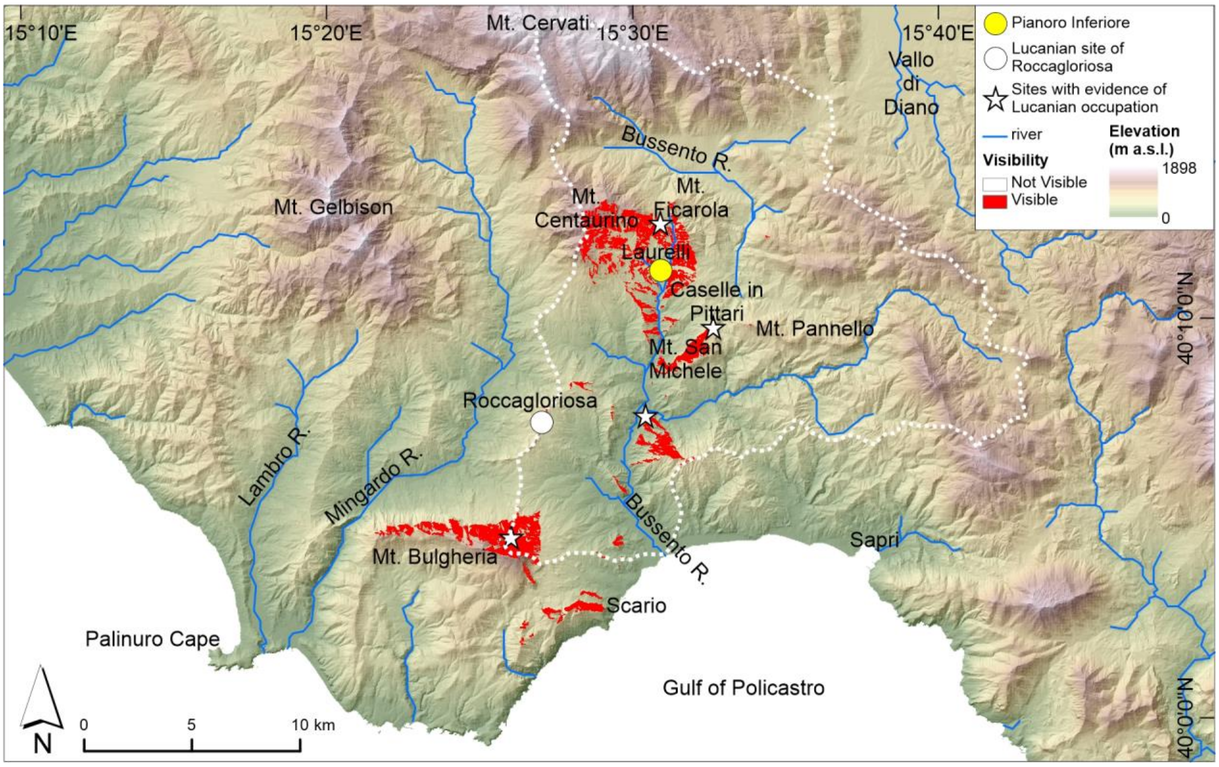

Figure 10. Visibility map from the Pianoro Inferiore. The dotted white line indicates the hydrographic basin of the Bussento River. Sites marked as showing evidence of occupation in Lucanian times derive from unpublished research carried out by the authors.

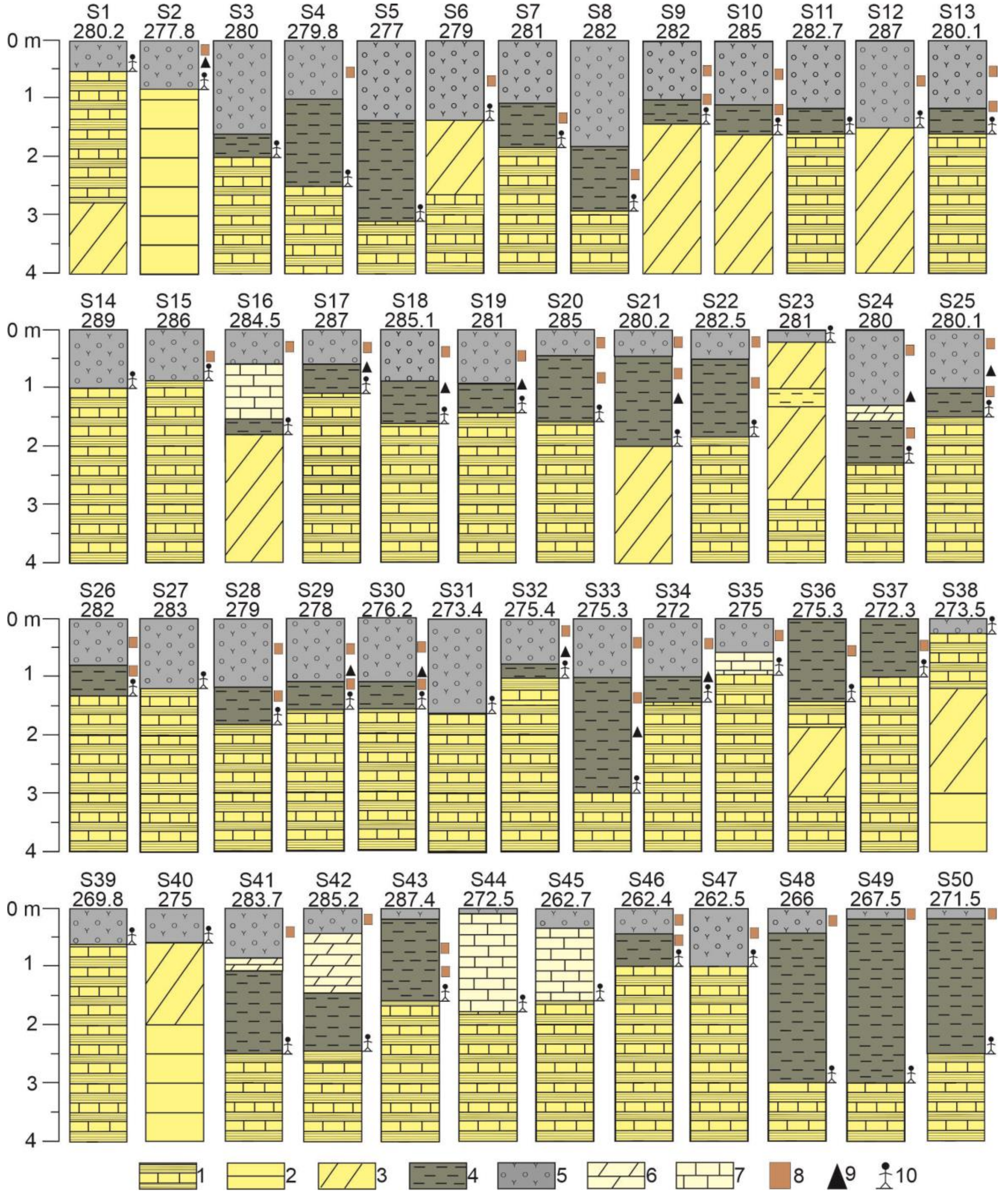

Figure 11. Logs of the fifty boreholes from the Laurelli site (for core locations see Figure 6). For each borehole, the top altitude is indicated in meters above sea level. Quaternary bedrock: 1—yellowish dense sands from very weathered sandstone boulders alternated with silty-clayey levels; 2—whitish dense sands from very weathered sandstone boulders; 3—yellowish dense sands from very weathered sandstone boulders. Historical deposits: 4—colluvial deposits with frequent presence of reworked ceramic sherds and carbonization traces; 5—soil. Archaeological evidence: 6—wall collapse; 7—wall structure; 8—ceramic sherds; 9—carbonization traces; 10—occupation level.

4.4. Archaeobotanical Record

A total of 106 wood fragments and two seeds were recovered (Table 1) in the analysed samples. Ten anthracological fragments were found in US 1085, nine of which were of hornbeam wood (*Ostrya/Carpinus*) (Figure 12a) and one of which was of vine (*Vitis vinifera* L.). The hornbeam wood fragments show a highly vitrified structure and are particularly hard when cut, which may indicate direct contact with fire. The vine wood fragment pertains to a twig in a fair condition of preservation. All the fragments related to the mopping up of trench 7 correspond to olive wood (*Olea europaea* L.) (Figure 12b).

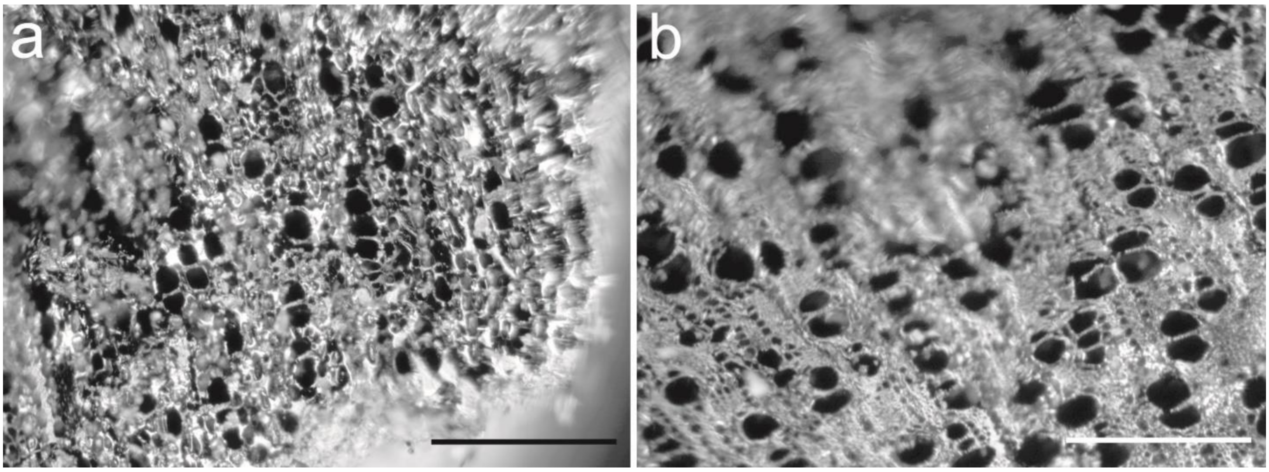

Figure 12. rLM images of the transverse sections of the two main species identified in the samples. (**a**) *Ostrya/Carpinus*; (**b**) *Olea europaea*. Scale bar 1 mm.

Under microscopic observation, they appear to be in fair condition of preservation, and the presence of ash and some vitrified parts are noticed in a few of the samples. Among the anthracological fragments found in UUSS 1098, 1107 and 1104, three are twigs: two in US 1104 and one in US 1198. All the fragments were identified, and all belong to olive wood. The fragments are in a fair condition of preservation and show traces of ash; particularly, the remains from US 1104 show traces of vitrification. Two charred seeds were collected from US 1107 and are identified as olive endocarps, one intact and one fragmented. The anthracological fragments relevant to US 1125 come from samples collected at different depths, of which there are thirty-three in total. The single charred wood fragment recovered at –18 cm was extremely vitrified, making taxonomic identification impossible. Among the 16 wood fragments found at −23 cm, 11 pertain to hornbeam wood and 5 are so vitrified that the anatomical elements necessary for identification are compromised. Two out of four wood fragments recovered at −26 cm could be recognized and identified as hornbeam wood; all fragments found at −32 cm were very vitrified, but all allowed for the recognition of the anatomical elements necessary for their attribution as hornbeam wood. Finally, the single fragment recovered at −65 cm was highly consumed and the anatomical elements necessary for identification could not be recognized.

4.5. The Iron-Rich Slags in the Archaeological Site

The slags considered in the present study are shown in Figure 13A–D. They are all deeply red-brown coloured and strongly heterogeneous, locally featuring dark-grey to blackish nuclei (inner parts) and vesiculated areas (i.e., Figure 13A). Concretions and deep red encrustations are also observed, as well as smaller whitish parts. Observed at OM under reflected light (Figure 14), the samples show microstructures with wüstite in mainly dendritic and globular habits (Figure 14A–D,F); this mineral is associated with olivine (fayalite) crystals in a glassy matrix (Figure 14A–C). Rare whitish droplets (Figure 14D,E) are interpreted as metallic iron (see SEM-EDS). The main mineral components recognized via combined XRPD and SEM-EDS analyses are reported in Table 2. Bulk XRPD analyses revealed that they are mainly composed of complex mixtures of iron-rich minerals. Very subordinated amounts of hematite, magnetite, rozenite and amarillite have been found; quartz, feldspar and amorphous component were also detected.

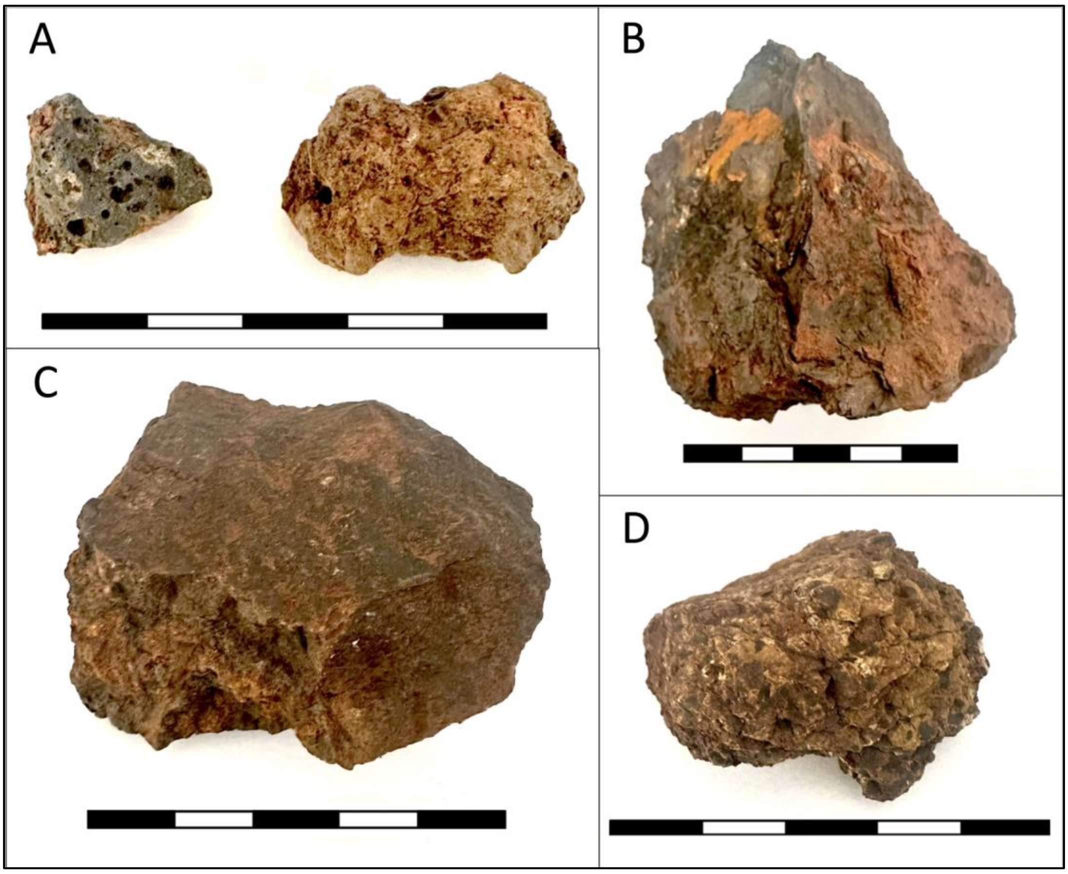

Figure 13. The four samples of iron-rich slags. (**A**) Sample CIP 1; (**B**) Sample CIP 2; (**C**) Sample CIP 5; (**D**) Sample CIP 6 (scale bar 5 cm).

Table 2. List of main phases and their ideal formulas observed in the investigated samples, inferred via XRPD and SEM-EDS. (x = present; blank = not detected).

Phase	Ideal Formula	XPRD	SEM-EDS
wüstite	FeO	x	x
olivine	$(Mg,Fe)_2SiO_4$	x	x
goethite	$FeO(OH)$	x	x
hematite	Fe_2O_3	x	
magnetite	$Fe^{2+}Fe^{3+}{}_2O_4$	x	
rozenite	$Fe^{2+}(SO_4)\cdot 4H_2O$	x	
amarillite	$NaFe^{3+}(SO_4)_2\cdot 6H_2O$	x	
iron	Fe		x
quartz	SiO_2	x	x
feldspar	$(K,Na)AlSi_3O_8$	x	x
leucite	$KAlSi_2O_6$		x
fluorapatite	$Ca5(PO_4)_3F$		x
galena	PbS		x
glassy matrix		x	x

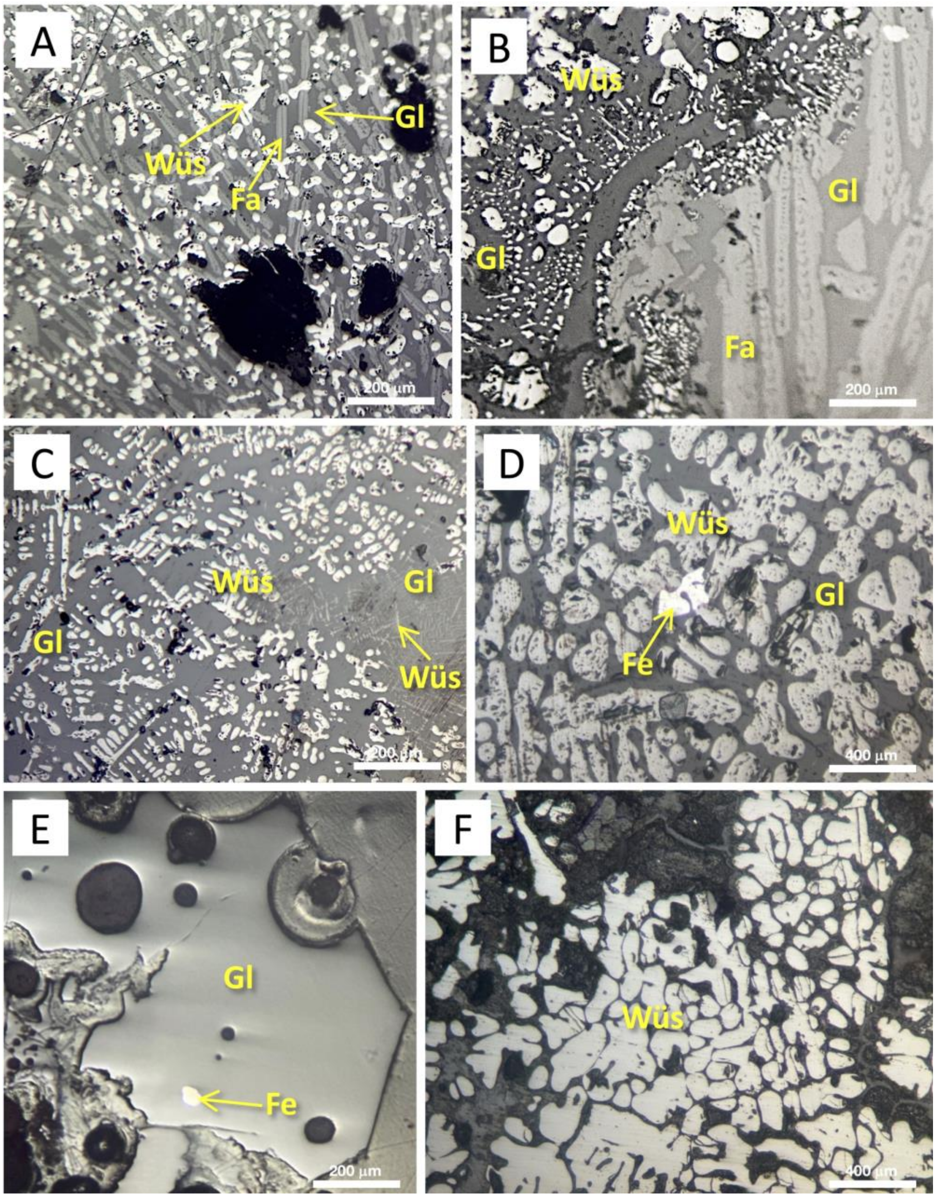

Figure 14. OM micrographs in reflected light of the investigated slags (P//). (**A**,**B**) Sample CIP 1; (**C**,**D**) Sample CIP 2; (**E**) Sample CIP 5; (**F**) Sample CIP 6. The white dendrites mainly consist of wüstite. The light grey crystals in (**A**,**B**) are fayalitic olivine. The white inclusions in (**D**,**E**) are metallic iron. Most of the other grey-coloured areas consist of a glassy matrix. Abbreviations: Fa, fayalitic olivine; Fe, metallic iron; Gl, glass; Wüs, wüstite.

Figures 15–19 show representative images of the samples using SEM-EDS. Quantitative EDS analyses carried out on selected minerals, as well as the amorphous matrix, are reported in Table 2. In sample CIP 1 (Figure 15A–H), elongated and dendritic fayalitic olivine crystals occur along with wüstite (Table 2) as rounded grains of various size in a glassy matrix, as confirmed by the elemental maps (Figure 15B–F). The glassy matrix is mainly composed of Si, Al, Fe, Mg, Ca, Na and K (with subordinated amounts of Ti and P), as shown in Table 2. Furthermore, in this matrix it was possible to see a black-coloured Si-K-Al-bearing pocket with white wüstite droplets (corresponding to the red frame in Figure 15A). We were not able to obtain reliable quantitative analyses of the black phase; however, this microstructure might correspond to a typical eutectoid wüstite-leucite microstructure observed in Roman slag [46]. In sample CIP 1, concretions of Fe oxy-hydroxides are also detected (Figure 16A), which can contain variable amounts of Mn (see the EDS spectra in Figure 16B,C); XRPD and chemical analyses revealed goethite to be the main component (Table 3). The same assemblage with Fe-(Mn) oxy-hydroxides is found in a colloform microtexture with bands and concentric layers of sample CIP 2 (Figure 17A–C); small quartz grains are also observed (Figure 17D).

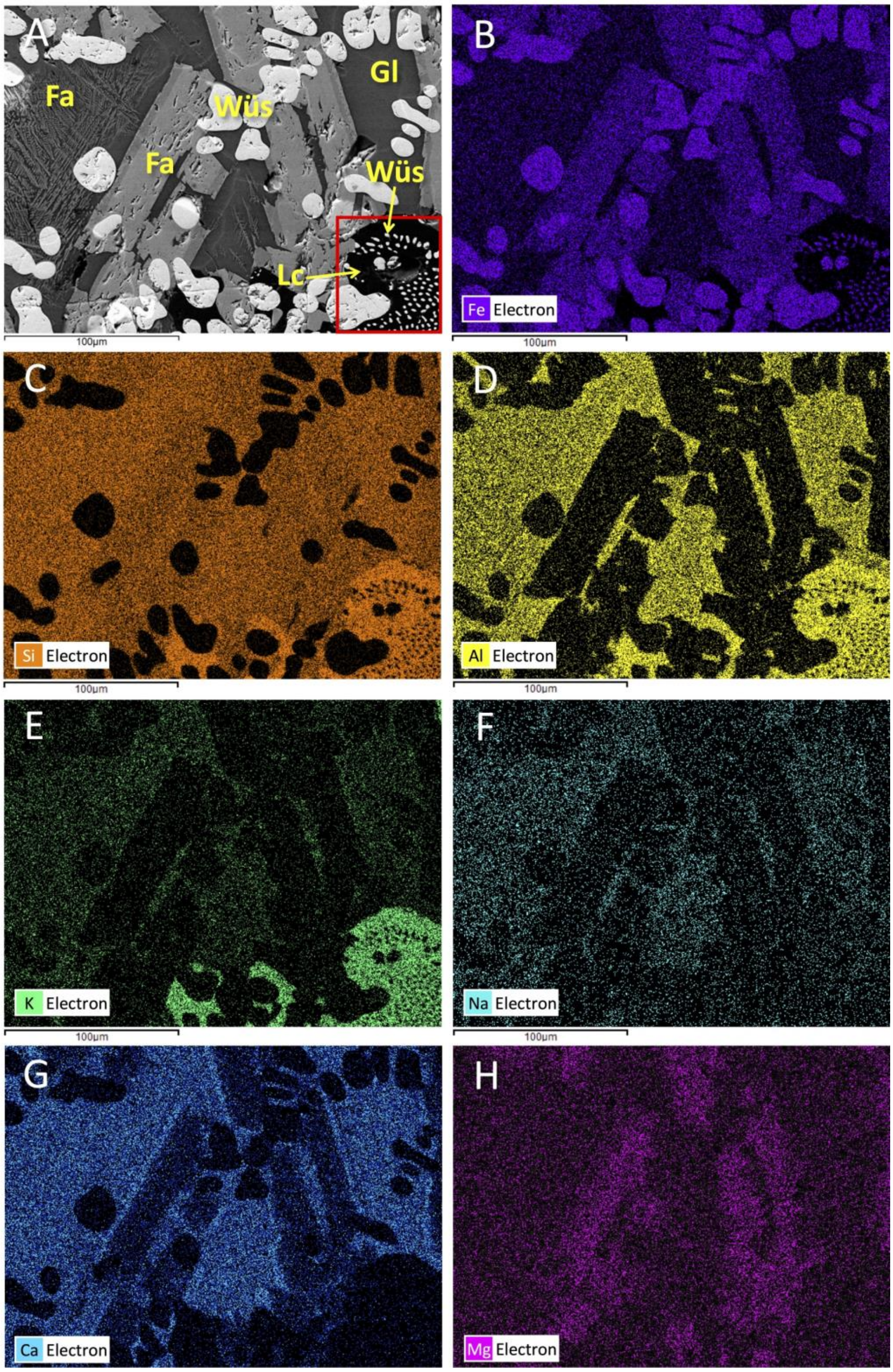

Figure 15. (**A**) BSE micrograph of sample CIP 1, showing elongated and dendritic fayalite with rounded grains of wüstite in a glassy matrix. See text for explanation of the mineral components in the red frame. (**B**–**H**) Selected elemental maps of the same area in (**A**). Abbreviations: Fa, fayalitic olivine; Fe, metallic iron; Gl, glass; Lc, leucite; Wüs, wüstite.

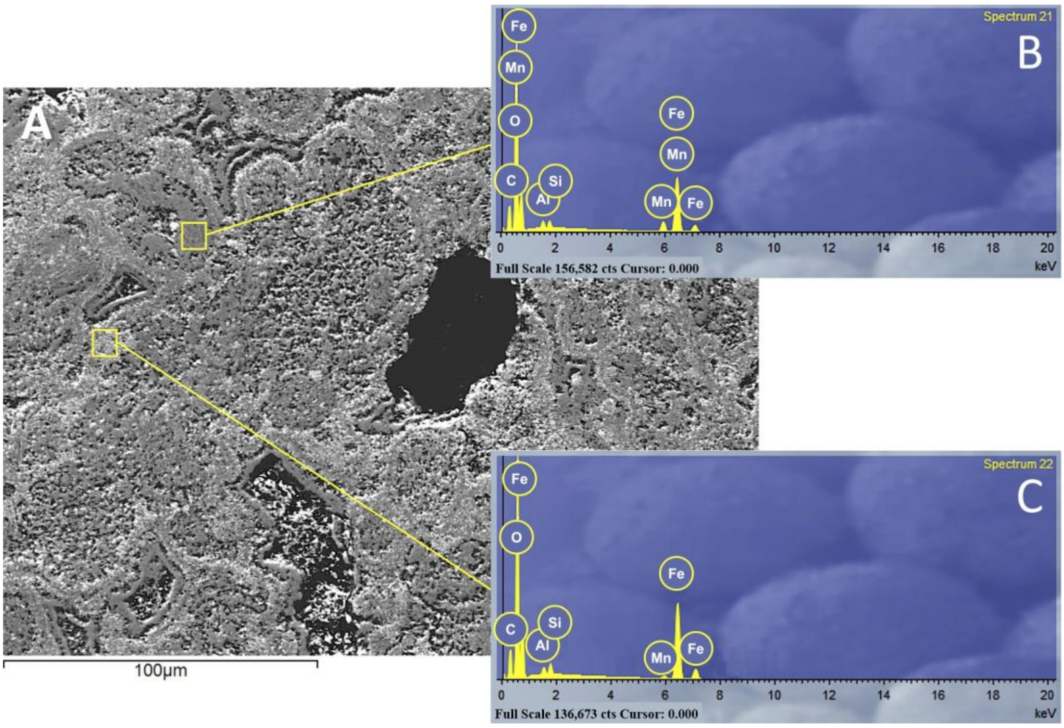

Figure 16. (**A**) BSE micrograph of sample CIP 1 of Fe-(Mn) oxy-hydroxides-bearing concretions. (**B**), (**C**) EDS spectra of Fe oxy-hydroxides with greater (darker areas) and lesser (lighter areas) Mn amounts, respectively.

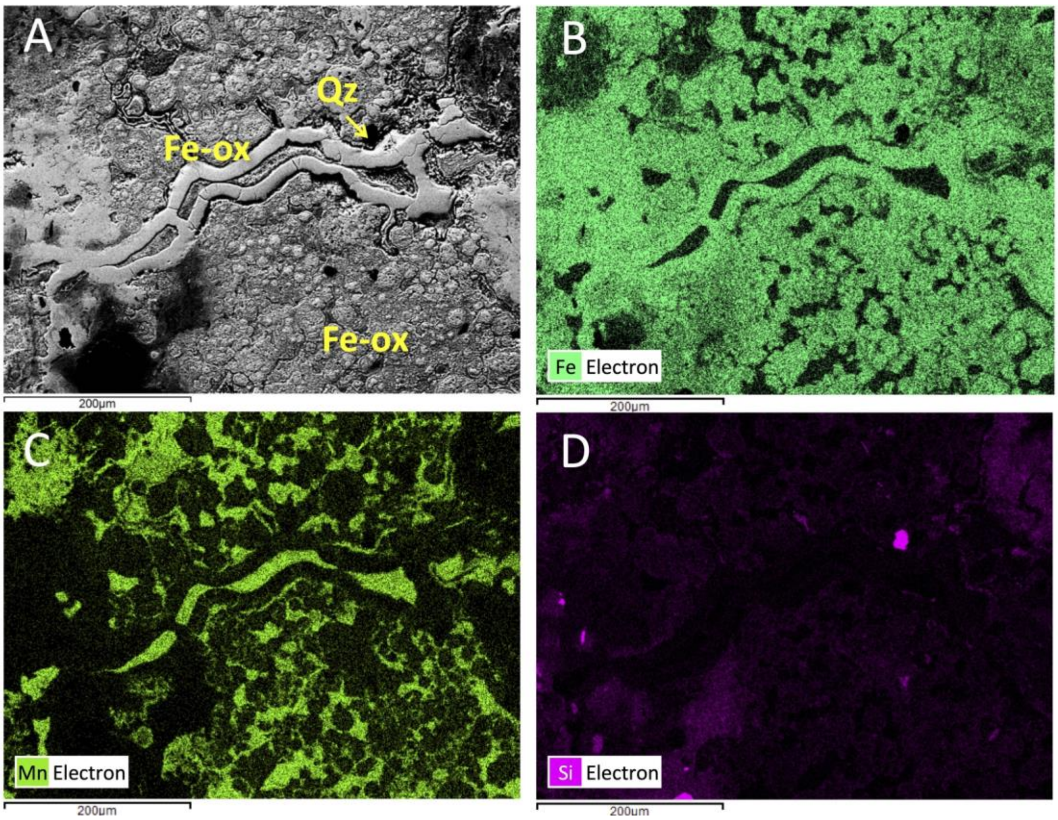

Figure 17. (**A**) BSE micrograph of sample CIP 2. (**B**–**D**) Selected elemental maps of the same area in (**A**), showing Fe-Mn oxy-hydroxides bearing concretions, as well as small quartz grains.

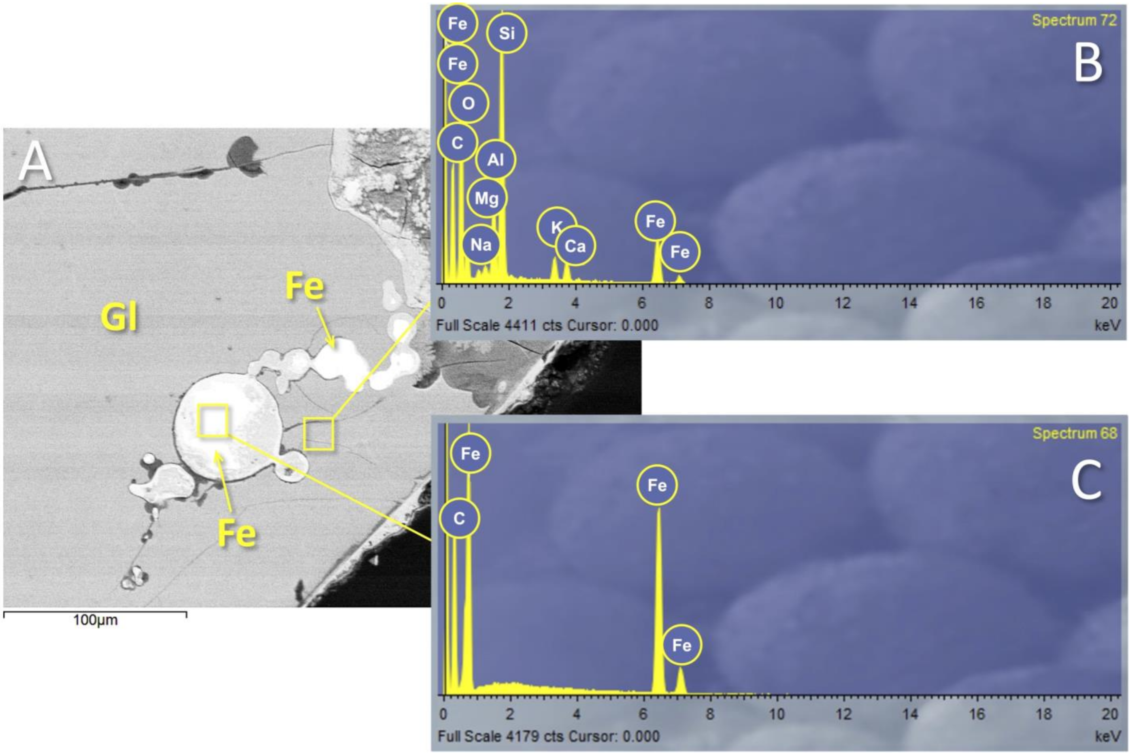

Figure 18. (**A**) BSE micrograph of sample CIP 5 of glassy material and metallic iron (lower EDS spectrum). (**B**) EDS spectrum of glass-rich area. (**C**) EDS spectrum of metallic iron in (**A**). Abbreviations: Fe, metallic iron; Gl, glass.

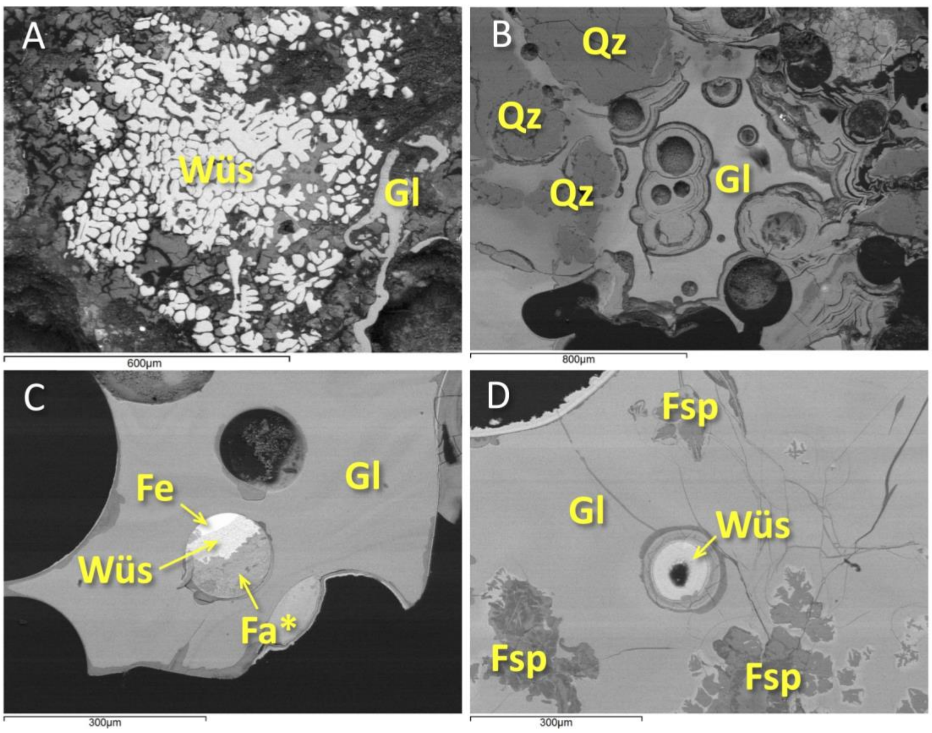

Figure 19. BSE micrographs of sample CIP 6. (**A**) Wüstite dendrites; (**B**) vesiculated glassy matrix with quartz grains (upper left side); (**C**) iron-wüstite cavity lining in glassy matrix; the darker part in the circular cavity, indicated with Fa*, refers to an olivine-like phase (its chemical analysis was not reliable). (**D**) Wüstite as cavity lining in glassy matrix, with feldspars aggregates (dark grey-colored crystals). Abbreviations: Fa*, fayalite-like phase; Fe, metallic iron; Fsp, feldspar; Gl, glass; Qz, quartz; Wüs, wüstite.

Table 3. Chemical composition of main phases found in the investigated slags.

	Wüstite			**Olivine**				**Goethite**			**Feldspar**		**Glassy Matrix**				
SiO_2					25.66	24.67			3.22	2.30	64.75	65.94	44.97	22.58	13.02	12.82	44.81
Al_2O_3								1.17	0.66	0.55	18.61	18.93	11.80	15.18	2.81	14.38	12.01
TiO_2					0.34	0.09							0.45	0.68		0.40	0.41
FeO	95.20	91.84	94.01		69.12	67.37		86.20	80.00	74.09		0.44	18.60	31.96	59.56	45.96	29.24
MnO								0.55									
MgO					2.34	3.09		1.93					2.52				1.83
CaO						1.19							11.78				5.17
Na_2O											2.34	3.27	1.63				1.59
K_2O											12.85	9.91	6.46				3.02
P_2O_5													0.65	1.21		2.77	
SO_3										0.54							
Cl																	
F																	
Total	95.20	91.84	94.01		97.46	96.41		89.85	83.88	77.48	98.55	98.49	98.86	71.61	75.39	76.34	98.08
	Iron					**Galena**											
Fe	98.80	97.29	100.99	99.94		2.19	1.55										
Ni		0.33															
Pb						79.81	85.32										
S						14.95	12.61										
Total	98.80	97.62	100.99	99.94		96.95	99.48										

In Figure 18A–C, the glassy matrix of sample CIP 5 shows some rounded vesicles, which are mainly filled with metallic iron (white part) and wüstite (light grey) (Table 2).

Sample CIP 6 shows dendritic wüstite in the glassy matrix (Figure 19A); a highly vesiculated glassy matrix with quartz grains is also found (Figure 19B). A microstructure similar to that of sample CIP 5, shown in Figure 18, is also seen (Figure 19C), whereas wüstite filling a vesicle in the glassy matrix with feldspar mineral aggregates can be seen in Figure 19D. Fluorapatite and galena were also observed in only two sites analysed using EDS (Tables 2 and 3).

5. Discussion

The Laurelli site represents one of the few examples of archaeological evidence of the Lucanian occupation in the Cilento, Vallo di Diano and Alburni Geopark. The results obtained through the above-described multidisciplinary approach have allowed for the addressing of different geoarcheological issues and open up new research lines.

5.1. The Spatial Setting of Laurelli

The geomorphological analysis of the Laurelli area highlighted the diffuse presence of landslides (Figure 7A), which is due to the sandy-clayey nature of the substrate (namely, the lower Cilento wedge-top units and the internal units; Figure 2). The occurrence of landslides is a common feature to many archaeological sites in the world [47–51]. In the Lucanian site of Roccagloriosa (see Figure 10 for reference), Ortolani and Pagliuca [52] have shown that landslides caused the abandonment of the town and covered the archaeological area by up to 3 m. This is supported by geological and geomorphological data coupled with the evidence of damages to buildings. In the coeval site of Laurelli, deep-seated landslides are widespread along the slopes of the Serrapotamo River basin, but they never directly affected the core areas of the Pianoro Inferiore. This is confirmed by geomorphological analysis, the nature and reduced thickness of the deposits covering the archaeological remains and by the lack of damages to the buildings. The different geomorphological setting of the archaeological sites of Roccagloriosa and Laurelli may explain the occurrence or absence of landsliding. Roccagloriosa was built on a roughly N–S oriented hill carved in limestone and marly-clayey rock types, which was affected by diffuse deep-seated landslides along its western and eastern slopes, up to the top of the hill [52]. Laurelli, in contrast, was founded on a large, low-relief depositional surface that was stable from a geomorphological point of view, making the site not prone to deep-seated landsliding.

Of note, stratigraphical data indicate that the thickness of the sediment cover increases towards the edge of the Pianoro Inferiore, i.e., close to the fluvial scarp of the Vallone Grande (Figure 6B). This local thickness increase may be related to alluvial events, in the form of hyperconcentrated flows, along the main valleys, possibly triggered by the reactivation of landslides to the north of Laurelli (i.e., the Caporra landslide, Figure 7A). These data suggest that despite the site of Laurelli did not suffer from deep landsliding, other natural events, such as hyperconcentrated flows or debris floods (sensu [53]), may have affected the areas overlooking the river valleys. Ongoing geomorphological investigations in the area hint at a possible interaction between the Caporra landslide system and the Pianoro Inferiore terrace, as previously suggested by Calcaterra et al. [45]. This implies that the Pianoro Inferiore edge could have experienced flooding due to the total or partial damming along the Vallone Grande creek after paroxysmal reactivations of the Caporra landslide system. This could be framed within climate-driven "geomorphological instabilities" during the so-called Archaic Little Ice Age of the 3rd century BCE [54,55]. At present, further investigations are needed to confirm or reject this hypothesis.

Other natural phenomena that may have caused the abandonment of the site are earthquakes. The analysis of recent [56] and historical [57,58] earthquake catalogues indicates that the epicentre of moderate to high magnitude earthquakes were not located in the surroundings of Laurelli in historical times. Thus, it is reasonable to hypothesize that the Pianoro Inferiore was chosen as the site to settle the town of Laurelli because it was a relatively stable surface. Furthermore, visibility analysis has shown that the Pianoro Inferiore is a strategic place as it allows for a visual connection with a large portion of the Serrapotamo River and the Bussento River valleys (Figure 10), thus favouring the control of a large part of this territory.

Based on subsurface data, it is also possible to identify on the Pianoro Inferiore the areas of greatest archaeological interest, which corresponds to the findings of wall structures in primary or collapsed positions. Interestingly, these finds appear to be scattered over the entire surface of the Pianoro Inferiore and are not concentrated in a single area, suggesting that the ancient settlement was as extensive as the entire surface. The analysis of unearthed structures indicates that the buildings were built with local rock types, mainly sandstones from Mt. Ficarola and Mt. Centaurino (Figure 2), and the Centola conglomerates.

Further indications come from the analysis of the colluvial sediment thickness (Figure 6B), which allows us to state that the original occupation level was slightly different from the present morphology. The different thickness of colluvial sediments visible in the map may be ascribed to natural transport and deposition by laminar runoff and to the presence of lower slope (terraced) areas separated by small escarpments.

The plant landscape in and around the town was not reconstructed because the analysis of archaeobotanical remains was very limited, leading to the identification of only two species: hornbeam and olive wood. Considering the contexts from which these remains were found, it is rather probable that the only fragments with an archaeological value are those related to hornbeam wood. This is supported by the features of the sediment in which they were found, as it was very compact, and the remains were almost integrated within the sediment (US 1125—trench 7). In fact, the interpretation of this layer as the level of the working phases of a metallurgical workshop aligns well with the possibility of using a specific type of wood. Furthermore, the use of hornbeam wood as fuel is well known in archaeology and it is one of the most common secondary woods for this purpose [59]. Additionally, the high vitrification and the presence of ash found on the samples suggest direct contact with fire, supporting the hypothesis of its use as fuel for processing. The other identified hornbeam wood fragments come from US 1085, a layer of the same trench. This stratum had evidently been reworked and it is quite possible that it contained some elements from US 1125. Concerning the olive wood fragments and seeds, it is very likely that they are intrusive elements. In fact, the layers in which these were identified mostly pertain to collapses or disturbed situations. The presence of vitrification and traces of ash on the samples can be explained by the possibility that they are residual fragments from fire events (natural or anthropogenic) that involved the olive trees that are still present in the surroundings of the excavation area. However, it cannot be ruled out that this species may also have been used as fuel in the past, as is well documented in the literature [60]. Nevertheless, the tree species identified in the anthracological record correspond with the environmental data of the local vegetation of the site [61,62].

5.2. First Achaeometric Data on Iron Slag Fragments

Preliminary investigations into the selected iron-rich slags indicate that they are basically composed of complex mixtures of Fe-bearing minerals (metallic iron, oxides, hydroxides, silicates and trace of sulfates), quartz, feldspar and silicate glassy matrix. As regards the silicate assemblage, it cannot be ruled out that further investigations may reveal the presence of minor contents of other silicates (i.e., clinopyroxene, kirschsteinite, etc.).

Ancient iron production involved a multi-step process (i.e., [63,64] and references therein). Iron ore, commonly derived from iron oxides, was first roasted to remove impurities and then heated in a closed furnace with charcoal. This process, known as direct or bloomery smelting, converted the ore (by CO in the furnace) into a porous mass of iron and impurities called a bloom. Only a small portion of the ore became iron, with the rest turning into slag. The bloom contained various substances, like silica and alumina, along with unreduced iron oxides and charcoal. Subsequently, the bloom was refined by heating and hammering to remove impurities and shape it into a finished product. As reported by Portillo et al. [64], this process involved two stages, i.e., heating in a hearth and hammering on an anvil. Due to various pyrometallurgical processes, two main types of slag are formed: smelting slag, which is the waste material from the ore, and smithing slag, which accumulates in the hearth. Both types produce numerous silicate slags, and their distinction is often tricky.

Considering the mineralogical assemblages and the petrographic and mineralogical features of the investigated samples, and by comparison with the literature ([46,64] and references therein), the studied slags might correspond to metallurgical wastes from smithing furnaces.

The presence of wüstite indicates furnace temperatures between 560 °C and 1200 °C, whereas olivine can indicate temperatures between 1000 and 1100 °C [64–67]. In order to determine more precisely the conditions in which the metallurgical process was performed, further mineralogical vs. petrographic investigations are in progress. Regarding the materials used as flux to decrease the iron melting point, mineralogical analyses show that quartz is quite widespread, while Ca is present only in small amounts in the various phases, suggesting that silica could probably be added as a flux, rather than lime.

Considering the small amounts of sulfur-bearing minerals found in the investigated slag material, it could be hypothesized that local mineralizations rich in Fe oxide-hydroxides were used as the raw material in iron production. Nevertheless, further analyses are required in order to better characterize the mineralogical, petrographic and geochemical features of the slags, as well as to clarify the source of the metal. Iron has been found in the so-called "House with the Metallurgical Workshop" (see Section 2.2). Archaeological analysis has not clarified whether this building was a workshop or a house-workshop with a space reserved for production activities. If the latter hypothesis were verified, this would represent an element of similarity with the coeval site of Roccagloriosa, where house-workshops for iron production have been found ([35] and references therein). Further archaeometric analysis on iron-rich rock types are underway to determine where the iron was extracted from (these samples are from the north-western side of Mt. San Michele, 40°09′49.2″ N, 15°32′28.3″ E, see Figure 2 for location). Results of these analyses will confirm whether or not local rock types were used for iron production, and this would have implications for the reconstruction of commercial routes. In the town of Velia (see Figure 1 for location), an important archaeological site of the CVDA Geopark, it has been proven that iron came from the Elba Island in central Italy [68]. The presence of workshops for iron production has also been demonstrated in other pre-Roman sites of southern Italy, such as Taranto in Puglia, Metaponto and Eraclea in Basilicata and Caulonia, Locri and Crotone in Calabria ([35] and reference therein). The continuation of this research will help in answering these still open questions about iron production.

6. Conclusions

The integrated geoarchaeological investigation of the site of Laurelli provides the first comprehensive picture of this ancient Lucanian town, which was founded in the 4th century BCE on a large, low-relief surface locally named the Pianoro Inferiore. The site where the town was settled was chosen because it is a stable area that is naturally protected by two stream valleys. Geomorphological and stratigraphical data suggest that landslides did not affect the Pianoro Inferiore, but it cannot be ruled out that hyperconcentred flows along the river valleys may have caused the accumulation of alluvial deposits in the peripheric part of the town. Further analyses are needed to confirm or to reject these hypotheses.

Archaeological surveys and the preliminary archaeometric analysis of iron-rich slags found there show that the city was a site of iron production. The fuel used in the furnace was, at least partially, represented by hornbeam wood, identified through anthracological analysis, and certainly harvested in the surrounding forests, where this species is still present. To investigate the potential geological provenance of the iron-rich material used in metallic artifacts at the Laurelli site, samples were collected from nearby outcrops. These outcrops contain levels and nodules within carbonate rocks characterized by a deep red-brown hue. Composed primarily of iron oxyhydroxides, these materials are currently undergoing mineralogical, petrographic, and geochemical analyses to determine if they could have served as the original metal source.

The study presented here represents a first step in understanding the history of this large pre-Roman archaeological site. Additional surveys and sampling will be conducted in the near future in parallel with the progress of archaeological excavations, aimed at better clarifying the selection and origin of raw materials used at the site. We are also confident that such a geoarchaeological analysis, along with the diffusion of this research, may have some benefit in terms of increasing the geotourism attractiveness of the Middle Bussento Karst System geosite.

Author Contributions: Conceptualization, E.V.; methodology, E.V., E.R.E., C.C., G.B., A.D.B. and C.G.; software, E.V.; validation, E.V., D.G. and E.R.E.; formal analysis, A.S., M.S., M.L.R., C.S. and M.V.; investigation, E.V., E.R.E., C.C., A.S., M.L.R., M.S., C.S., D.G., G.B., A.D.B. and C.G.; data curation, E.V.; writing—original draft preparation, E.V., E.R.E., C.C., A.S., M.L.R., M.S., C.S., D.G., M.V., G.B., A.D.B. and C.G.; writing—review and editing, E.V., D.G., E.R.E. and G.B.; visualization, E.V., D.G., E.R.E. and G.B.; supervision, E.V., D.G., E.R.E. and G.B. All authors have read and agreed to the published version of the manuscript.

Funding: G.B. has benefited from the research fund "Ricerca Diparimentale 2020–2021" granted by the University of Naples Federico II (Naples, Italy).

Data Availability Statement: The raw data supporting the conclusions of this article will be made available by the authors on request.

Acknowledgments: These archaeological investigations are conducted under ministerial concession no. 673 of 30 May 2022. We wish to thank the Academic Editor and the reviewers whose comments helped us to improve the manuscript. We would thank the Soprintendenza Archeologia, belle arti e paesaggio per le province di Salerno e Avellino for providing logistic support for the geoarchaeological analysis. We thank the mayor, the town council, and the entire community of Caselle in Pittari for their support during the archaeological excavation activities. We would also like to thank Fausto Longo, director of the Or-Sa inter-university specialization school, for his continuous support.

Conflicts of Interest: The authors declare no conflicts of interest.

References

1. Valente, E.; Santo, A.; Guida, D.; Santangelo, N. Geotourism in the Cilento, Vallo di Diano and Alburni UNESCO Global Geopark (Southern Italy): The Middle Bussento Karst System. *Resources* **2020**, *9*, 52. [CrossRef]
2. Eder, F.W.; Patzak, M. Geoparks—Geological attractions: A tool for public education, recreation and sustainable economic development. *Episodes* **2004**, *27*, 162–164. [CrossRef] [PubMed]
3. UNESCO Global Geopark Definition. Available online: http://www.globalgeopark.org/aboutGGN/6398.htm (accessed on 3 November 2024).
4. Santangelo, N.; Santo, A.; Guida, D.; Lanzara, R.; Siervo, V. The geosites of the Cilento-Vallo di Diano national park (Campania region, southern Italy). *Il Quat.* **2005**, *18*, 101–112.
5. Santangelo, N.; Romano, P.; Santo, A. Geo-itineraries in the Cilento Vallo di Diano Geopark: A Tool for Tourism Development in Southern Italy. *Geoheritage* **2015**, *7*, 319–335. [CrossRef]
6. Santangelo, N.; Amato, V.; Ascione, A.; Russo Ermolli, E.; Valente, E. GEOTOURISM as a Tool for Learning: A Geoitinerary in the Cilento, Vallo di Diano and Alburni Geopark (Southern Italy). *Resources* **2020**, *9*, 67. [CrossRef]
7. Valente, E.; Casaburi, A.; Finizio, M.; Papaleo, L.; Sorrentino, A.; Santangelo, N. Defining the Geotourism Potential of the Cilento, Vallo di Diano and Alburni UNESCO Global Geopark (Southern Italy). *Geosciences* **2021**, *11*, 466. [CrossRef]
8. Parco Paestum e Velia. Available online: https://museopaestum.cultura.gov.it/al-parco-archeologico-di-paestum-e-velia-record-assoluto-di-visitatori-nellanno-2023/ (accessed on 5 November 2024).
9. Cilento, Vallo di Diano and Alburni Geopark Geosites Database. Available online: https://www.cilentoediano.it/il-parco-nazionale/geologia-e-geomorfologia/ (accessed on 5 November 2024).
10. Amato, V.; Di Paola, G.; Rosskopf, C.M.; Avagliano, G.; Cipriani, M.; Cinque, A.; Pontrandolfo, A.; Santoriello, A. Geomorphology and geoarchaeology of the Paestum area: Modifications of the physical environment in historical times. *Mediterranee* **2009**, *112*, 129–135. [CrossRef]
11. Cozzolino, M.; Longo, F.; Pizzano, N.; Rizzo, M.L.; Voza, O.; Amato, V. A Multidisciplinary Approach to the Study of the Temple of Athena in Poseidonia-Paestum (Southern Italy): New Geomorphological, Geophysical and Archaeological Data. *Geosciences* **2019**, *9*, 324. [CrossRef]
12. Amato, V.; Anzalone, E.; Aucelli, P.P.C.; D'Argenio, B.; Ferreri, V.; Rosskopf, C.M. Sedimentology and depositional history of the travertines outcropping in the Poseidonia-Paestum archaeological area. *Rend. Fis. Acc. Lincei* **2012**, *23*, 61–68. [CrossRef]
13. Amato, V.; Cicala, L.; Valente, E.; Ruello, M.R.; Esposito, N.; Russo Ermolli, E. Anthropogenic amplification of geomorphic processes along the Mediterranean coasts: A case-study from the Graeco-Roman town of Elea-Velia (Campania, Italy). *Geomorphology* **2021**, 107694. [CrossRef]
14. Santangelo, N.; Daunis-i-Estadella, J.; Di Crescenzo, G.; Di Donato, V.; Faillace, P.I.; Martín-Fernández, J.A.; Romano, P.; Santo, A.; Scorpio, V. Topographic predictors of susceptibility to alluvial fan flooding, Southern Apennines. *Earth Surf. Process. Landf.* **2012**, *37*, 803–817. [CrossRef]
15. Budetta, P.; Santangelo, N.; Santo, A. Interazioni tra processi alluvionali ed insediamenti abitativi in epoca storica: Il caso della Certosa di Padula. In Proceedings of the Atti Convegno GeoBen, Turin, Italy, 7–9 June 2000; pp. 41–48.
16. Martini, I.; Ronchitelli, A.; Arrighi, S.; Capecchi, G.; Ricci, S.; Scaramucci, S.; Spagnolo, V.; Gambassini, P.; Moroni, A. Cave clastic sediments as a tool for refining the study of human occupation of prehistoric sites: Insights from the cave site of La Cala (Cilento, southern Italy). *J. Quanternary Sci.* **2018**, *3*, 586–596. [CrossRef]
17. Carmignani, M.; Martini, I.; Spagnolo, V.; Dominici, C.; Rossini, M.; Scaramucci, S.; Moroni, A. Middle and early upper Pleistocene human occupations in Southern Italy. A reassessment of the assemblages from Cala d'Arconte, Capo Grosso and Cala Bianca. *J. Archaeol. Sci. Rep.* **2021**, *40*, 103256. [CrossRef]
18. Mazzoli, S.; Helman, M. Neogene patterns of relative plate motion for Africa-Europe: Some implications for recent central Mediterranean tectonics. *Geol. Rundsch.* **1994**, *83*, 464–468. [CrossRef]
19. Turco, E.; Macchiavelli, C.; Mazzoli, S.; Schettino, A.; Pierantoni, P. Kinematic evolution of Alpine Corsica in the framework of Mediterranean mountain belts. *Tectonophysics* **2012**, *579*, 193–206. [CrossRef]
20. Cello, G.; Mazzoli, S. Apennine Tectonics in Southern Italy: A review. *J. Geodyn.* **1998**, *27*, 191–211. [CrossRef]
21. Menardi Noguera, A.; Rea, G. Deep structure of the Campanian–Lucanian Arc (Southern Apennine, Italy). *Tectonophysics* **2000**, *324*, 239–265. [CrossRef]
22. Vitale, S.; Ciarcia, S. Tectono-stratigraphic and kinematic evolution of the southern Apennines/Calabria–Peloritani Terrane system (Italy). *Tectonophysics* **2013**, *583*, 164–182. [CrossRef]
23. Ciarcia, S.; Vitale, S.; Di Staso, A.; Iannace, A.; Mazzoli, S.; Torre, M. Stratigraphy and tectonics of an Internal Unit of the southern Apennines: Implications for the geodynamic evolution of the peri-Tyrrhenian mountain belt. *Terra Nova* **2009**, *21*, 88–96. [CrossRef]
24. Ciarcia, S.; Mazzoli, S.; Vitale, S.; Zattin, M. On the tectonic evolution of the Ligurian accretionary complex in southern Italy. *Geol. Soc. Am. Bull.* **2012**, *124*, 463–483. [CrossRef]

25. Vitale, S.; Ciarcia, S.; Mazzoli, S.; Iannace, A.; Torre, M. Structural analysis of the 'Internal' Units of Cilento, Italy: New constraints on the Miocene tectonic evolution of the southern Apennine accretionary wedge. *CR Geosci.* **2010**, *342*, 475–482. [CrossRef]
26. Vitale, S.; Ciarcia, S.; Mazzoli, S.; Zaghloul, M.N. Tectonic evolution of the 'Liguride' accretionary wedge in the Cilento area, southern Italy: A record of early Apennine geodynamics. *J. Geodyn.* **2011**, *51*, 25–36. [CrossRef]
27. Sheet 520—Sapri of the Geological Map of Italy at Scale 1:50000, Carg Project. Available online: http://www.isprambiente.gov.it/Media/carg/520_SAPRI/Foglio.html (accessed on 6 November 2024).
28. Guida, D.; Guida, M.; Luise, D.; Salzano, G.; Vallario, A. Ricostruzione di sequenze morfoevolutive nell'area ad Ovest di Monte Sacro. *Geol. Appl. Ed Idrogeol.* **1980**, *XV*, 122.
29. Serritella, A. Recenti ricerche a Caselle in Pittari. In *Il Golfo di Policastro tra Enotri e Lucani: Insediamenti, Assetto Istituzionale, Cultura Materiale*; La Torre, G.F., Mollo, F., Eds.; Atti del Convegno Internazionale, Università degli Studi di Messina: Tortora, Italy, 2016; pp. 261–272.
30. Fiammenghi, C.A.; Salomone, F.; Serritella, A. Caselle in Pittari. In *Ricerche Sulla Casa in Magna Grecia e Sicilia*; D'Andria, F., Mannino, K., Eds.; Atti del Colloquio: Lecce, Italy, 1992; pp. 321–334.
31. Serritella, A. *Caselle in Pittari: Un Sito Lucano nell'Entroterra del Golfo di Policastro', in Oebalus*; Studi sulla Campania nell'Antichità: Rome, Italy, 2015; pp. 227–242.
32. Serritella, A. Abitare a Caselle in Pittari, Sezione tematica "Abitare in Magna Grecia. L'età classica". *AIONArchStAnt N.S.* **2022**, *29*, 247–257.
33. Serritella, A.; Rizzo, M.L. Nuove ricerche a Caselle in Pittari. *J. Fasti Online* **2019**, *439*, 1–11. Available online: https://www.fastionline.org/docs/FOLDER-it-2019-439.pdf (accessed on 15 November 2024).
34. Capozzoli, L.; De Martino, G.; Lapenna, V.; Perciante, F.; Rizzo, E.; Rizzo, M.L.; Serritella, A.; Scafuro, M.; Voza, O. Preliminary geophysical surveys and archaeological studies into the buried urban plan of the Lucanian settlement of Caselle in Pittari. In Proceedings of the IMEKO TC-4 MetroArchaeo, Trento, Italy, 22–24 October 2020.
35. Serritella, A.; Rizzo, M.L. Un'officina metallurgica a Caselle in Pittari. *Fasti Line Doc. Reserch* **2021**, *507*, 1–13.
36. Libero Mangieri, G. Un ripostiglio di monete magnogreche da Caselle in Pittari. *Ann. Dell'istituto Ital. Di Numis.* **1994**, *38–41*, 167–172.
37. Dramis, F.; Guida, D.; Valiante, M. Object-Oriented Mapping as a Tool for the Assessment of Landslide Hazard in Higly Urbanized Areas. *Front. Earth Sci.* **2022**, *10*, 834078. [CrossRef]
38. Valiante, M.; Di Benedetto, A.; Aloia, A. A Comparison of Landforms and Processes Detection Using Multisource Remote Sensing Data: The Case Study of the Palinuro Pine Grove (Cilento, Vallo di Diano and Alburni National Park, Southern Italy). *Remote Sens.* **2024**, *16*, 2771. [CrossRef]
39. Tarquini, S.; Isola, I.; Favalli, M.; Battistini, A.; Dotta, G. *TINITALY, a Digital Elevation Model of Italy with a 10 Meters Cell Size (Version 1.1)*; Istituto Nazionale di Geofisica e Vulcanologia (INGV): Rome, Italy, 2023. [CrossRef]
40. Greguss, P. Identification of Living Gymnosperms on the Basis of Xylotomy. Akadémiai Kiadó: Budapest, Hungary, 1955.
41. Schweingruber, F.H. *Anatomy of European Woods*; Verlag Kassel: Bern, Switzerland, 1990.
42. Vernet, J.L.; Ogereau, P.; Figueiral, I.; Machado Yanes, C.; Uzquiano, P. *Guide D'identification des Charbons de Bois Préhistoriques et Récents*; CNRS Éditions: Parigi, France, 2001.
43. Nardi Berti, R. *La Struttura Anatomica del Legno ed il Riconoscimento dei Legami Italiani di Più Corrente Impiego*; CNR, IVALSA: Trento, Italy, 2006.
44. Valiante, M.; Guida, D.; Della Seta, M.; Bozzano, F. Spatiotemporal data management of recurrent debris flow events using object-oriented data modelling. *Ital. J. Eng. Geol. Environ.* **2021**, *1*, 239–248. [CrossRef]
45. Calcaterra, D.; Guida, D.; Budetta, P.; De Vita, P.; Di Martire, D.; Aloia, A. Moving geosites: How landslides can become focal points in Geoparks. *Latest Trends Eng. Mech. Struct. Eng. Geol.* **2014**, *2*, 162–171.
46. Kramar, S.; Tratnik, V.; Hrovatin, I.M.; Mladenovic, A.; Pristacz, H.; Rogan Smuc, N. Mineralogical and chemical characterization of Roman slag from the archaeological site of Castra (Ajdovscina, Slovenia). *Archaeometry* **2015**, *57*, 704–719. [CrossRef]
47. Delmonaco, G.; Margottini, C.; Orlando, L.; Spizzichino, D. Integration of geophysical investigation to landslide analysis in the archaeological site of Stabiae (Italy). In *Landslide Science and Practice, Risk Assessment, Management and Mitigation*; Margottini, C., Canuti, P., Sassa, K., Eds.; Springer: Berlin/Heidelberg, Germany, 2013; Volume 6, pp. 561–569.
48. Garduño-Monroy, V.H.; Macías, J.L.; Morelli, S.; Figueroa-Soto, A.; Ruiz-Figueroa, A.; Robles-Camacho, J.; Veronica, P. Landslide impact on the archaeological site of Mitla. Oaxaca. *Geoarchaeology* **2020**, *35*, 644–658. [CrossRef]
49. Marinos, P.; Rondoyanni, T. The Archaeological Site of Delphi, Greece: A Site Vulnerable to Earthquakes, Rockfalls and Landslides. In *Landslides*; Sassa, K., Fukuoka, H., Wang, F., Wang, G., Eds.; Springer: Berlin/Heidelberg, Germany, 2005.
50. Pappalardo, G.; Imposa, S.; Barbano, M.S.; Grassi, S.; Mineo, S. Study of landslides at the archaeological site of Abakainon necropolis (NE Sicily) by geomorphological and geophysical investigations. *Landslides* **2018**, *15*, 1279–1297. [CrossRef]

51. Spizzichino, D.; Margottini, C.; Puzzilli, L.M. Landslide Risk Assessment and Management in the Archaeological Site of Machu Picchu (Peru). In *Proceedings of the Geotechnical Engineering for the Preservation of Monuments and Historic Sites*; Bilotta, E., Flora, A., Lirer, S., Viggiani, C., Eds.; Taylor & Francis Group: Abingdon, UK, 2013; pp. 697–707.
52. Ortolani, F.; Pagliuca, S. Caratteristiche geologiche ed evoluzione geomorfologica olocenica dell'area archeologica di Roccagloriosa (Cilento, Campania). *Mem. Della Soc. Geol. Ital.* **1989**, *42*, 53–60.
53. Hungr, O.; Leroueil, S.; Picarelli, L. The Varnes classification of landslide types, an update. *Landslides* **2014**, *11*, 167–194. [CrossRef]
54. Ortolani, F.; Pagliuca, S. Variazioni climatico-ambientali nel periodo storico nell'area mediterranea: Evidenze geoarcheologiche di cicliche crisi ambientali tipo "effetto serra". In Proceedings of the Atti del Convegno "Il Ruolo della Geomorfologia nella Geologia del Quaternario", Napoli, Italy, 27–29 February 1996.
55. Ortolani, F.; Pagliuca, S. Relazione tra clima, ambiente e attività solare negli ultimi millenni. Previsioni per il prossimo futuro. *Geol. Dell'ambiente* **2008**, *3*, 9–13.
56. ISIDe Working Group. Italian Seismological Instrumental and Parametric Database (ISIDe) (Version 1). Istituto Nazionale di Geofisica e Vulcanologia (INGV). 2007. Available online: https://terremoti.ingv.it/en/iside (accessed on 6 December 2024).
57. Rovida, A.; Locati, M.; Camassi, R.; Lolli, B.; Gasperini, P.; Antonucci, A. Catalogo Parametrico dei Terremoti Italiani (CPTI15), versione 4.0 [Data set]. Istituto Nazionale di Geofisica e Vulcanologia (INGV). 2022. Available online: https://emidius.mi.ingv.it/CPTI15-DBMI15/query_eq/ (accessed on 20 October 2024).
58. Rovida, A.; Locati, M.; Camassi, R.; Lolli, B.; Gasperini, P. The Italian earthquake catalogue CPTI15. *Bull. Earthq. Eng.* **2020**, *18*, 2953–2984. [CrossRef]
59. Veal, R. Fuelling Ancient Mediterranean Cities: A Framework for Charcoal Research. In *The Ancient Mediterranean Environment between Science and History*; Harris, W.V., Ed.; Brill Publishing: Laiden, The Netherlands; Boston, MA, USA, 2013; pp. 37–58. [CrossRef]
60. Rowan, E. Olive Oil Pressing Waste as a Fuel Source in Antiquity. *Am. J. Archaeol.* **2015**, *119*, 465–482. [CrossRef]
61. Pignatti, S. *Ecologia Vegetale*; Uted edizioni: Roma, Italy, 1995.
62. Pignatti, S. *Flora d'Italia vol I-II-III*; Edagricole: Bologna, Italy, 1982.
63. Giardino, C. *I Metalli nel Mondo Antico. Introduzione all'Archeometallurgia*; Manuali Laterza: Bari, Italy, 2017; p. 350, ISBN 9788842092018.
64. Portillo, H.; Zuluaga, M.C.; Ortega, L.A.; Alonso-Olazabal, A.; Murelaga, X.; Martinez-Salcedo, A. XRD, SEM/EDX and micro-Raman spectroscopy for mineralogical and chemical characterization of iron slags from the Roman archaeological site of Forua (Biscay, North Spain). *Microchem. J.* **2018**, *138*, 246–254. [CrossRef]
65. Caro, T.; Riccucci, C.; Parisi, E.I.; Renzulli, A.; Moro, S.; Santi, P.; Faraldi, F. Archaeometallurgical studies of tuyeres and smelting slags found at Tharros (north-western Sardinia, Italy). *Appl. Phys. A* **2013**, *113*, 933–943. [CrossRef]
66. Rocchi, I.; Masotta, M.; Rocchi, S. Petrology of iron and copper slags from historical smelting activity in southern Tuscany. *Period. Di Mineral.* **2023**, *92*, 57–73. [CrossRef]
67. Kostova, B.; Paneva, D.; Cherkezova-Zheleva, Z.; Mihaylova, K.; Dumanov, B. Ancient Metallurgical Iron Slags—Chemical, Powder X-ray Diffraction and Mössbauer Spectroscopic Study. *Crystals* **2023**, *13*, 888. [CrossRef]
68. Gassner, V. La produzione del ferro a Velia. In Proceedings of the Atti del II Convegno Internazionale "Dialoghi sull'Archeologia della Magna Grecia e del Mediterraneo", Paestum, Italy, 28–30 June 2017.